New superconducting phase in nuclei

O. Dumitrescu
Institute of Physics and Nuclear Engineering, Institute of Atomic Physics, Bucharest, Rumania

Fiz. Elem. Chastits At. Yadra **23**, 430–478 (March–April 1992)

The influence of pairing and dynamical α-type correlations on the structure of nuclear states is studied in the framework of the enlarged superfluid model. A new superfluid phase, the so-called α-like superfluid phase, is introduced. New types of isomers with corresponding bands of elementary excitations are predicted. The odd–even staggering of the charge radii of chains of isotopes of various nuclei is explained together with some other experimental data.

INTRODUCTION

Symmetries introduce beauty and order into physical phenomena and their mathematical description. Some can help us (and are often used as a tool) to hide the absence of a deeper understanding. However, they die if they are not changed. Moreover, if a symmetry is broken, then, as is well known in art or architecture, this creates life and gives new strength. For this reason, the breaking of a symmetry may give us more information about a physical system than if the symmetry were unbroken. The causal symmetry associated with the conservation of particle number was valid for a long time and therefore could be used as a restriction. The discovery of its violation became a great stimulus for experimental and theoretical investigations.

In 1958, Bohr, Mottelson, and Pines[1] pointed out a certain similarity between the structure of nuclei and the electron structure of metals. In particular, they emphasized the analogy between the energy gap which exists in the spectrum of intrinsic excitations of nuclei and the energy gap observed in an electron excitation of superconducting metals. Their paper opened up a very rich and general field of investigations between solid-state physics and nuclear physics; specifically, the two fields are united by the phenomenon of pairing. Application of this theory explains the energy gap in the spectrum of even–even nuclei, introduces a certain mixing of configurations near the Fermi surface, and shows how the nuclear moment of inertia decreases from the rigid-body value calculated in accordance with the Hartree–Fock model to the experimental value. Effective pairing and long-range interactions are studied in the framework of the random phase approximation (RPA), which, therefore, describes elementary collective excitations. In the framework of this approach, normal fluid nuclei are well separated from superfluid nuclei, and the transition between these two phases occurs in the second order.[2] Elementary single-quasiparticle and collective excitations will be described in the framework of the superfluid model for the quasiparticle–phonon nuclear model (QPNM)[3,4] when the investigated objects are superfluid nuclei. Such a model, which is good for heavy nuclei, has a shortcoming, since the possibility of formation of neutron–proton pairs is omitted from it. The argument for neutron–proton pairing correlations is particularly strong for light nuclei, in which the neutrons and protons occupy the same orbitals; however, the density of the single-particle levels is too low, and cases of superconducting light nuclei are not observed. Such correlations can be included in the framework of Hartree–Fock–Bogolyubov (HFB) theory and explain new phenomena that cannot be investigated by ordinary Hartree–Fock (HF) plus Bardeen–Cooper–Schrieffer (BCS)[5,6] theories. These include neutron–proton correlations, Coriolis antipairing, pair alignment, gapless superconductivity, shape transitions, coexistence of shapes, and branching of spectra. However, there exist experimental data relating to odd–even staggering of the charge radii of nuclei in chains of isotopes of various elements[7–12] that cannot be explained in the framework of HFB theory, which includes only the interaction of two nucleons.

Geometrical symmetries are used to describe special simple properties of complicated structures. Examples of geometrical symmetries associated with reflections and rotations can be seen in many objects, including nuclei. Dynamical symmetries are associated with relatively simple ordering, which can sometimes be discovered in the laws that govern the behavior of physical systems. Because of the complexity of the nuclear many-body problem, one cannot expect such symmetries to play a decisive role in nuclear physics. However, it has been shown that the arrangement and decay properties of the excited states of a large number of even–even nuclei can be correctly calculated by using a symmetry in which valence nucleons are paired with the formation of bosons with spin 0 and 2. Such a model, the interacting boson model (IBM) is characterized by a special picture of nuclear energy levels, which depends only on the number of bosons present.[13,14] This symmetry already ensures the unification of several different forms of nuclear collective motion (for example, rotation, vibration, and intermediate behavior of the system between these limiting cases). All these models can be described in a unified manner by the symmetry associated with the IBM, which depends simply on the number of valence interacting bosons present in each nucleus. Since the model is used in this manner to describe the collective characteristics and shell properties, one can hope to obtain a generalization of the shell and collective nuclear models.

 0090-4759/92/020187-23$04.00

The most recent achievements have been associated with enlargement of this model to odd and odd–odd nuclei. This enlargement includes coupling between unpaired nucleons and bosons (paired nucleons) in neighboring nuclei, permitting calculation of the properties of nuclear states, for example, in odd and even–even nuclei by means of a simple formula, as in the QPNM. This coupling is characterized by supersymmetry. However, in contrast to the IBM, which has had tremendous success in a wide range of even–even nuclei, there are as yet only a few successful examples of supersymmetry, while for nuclei which are only slightly removed from this region there exists a serious discrepancy with the supersymmetry predictions. At the present time it is not clear what is the origin of the problem: Is it in the supersymmetric model and its calculations or in the inability to analyze and generalize experimental results in a way that reveals the expected supersymmetric picture? At the least, it is known that unpaired nucleons can change the symmetry properties of an even–even core.

To eliminate some shortcomings of the QPNM compared with the IBM, we included[15–18] additionally a four-nucleon (proton-pair–neutron-pair) effective residual interaction. This model—the enlarged superfluid model (ESM)—makes it possible to consider new phenomena that cannot be investigated in the QPNM, HFB approach, and IBM, for example: 1) superfluidity of the neutron and proton systems in the region of heavy nuclei (rare earths and actinides); 2) enrichment of the phase structure by a new superfluid phase dominant in α-particle correlations; 3) new predicted first- and second-order phase transitions; 4) new predicted isomers (so-called superfluid isomers) with corresponding bands of elementary excitations. The inducing of superfluidity from the neutron to the proton system and vice versa is the key to the explanation of the odd–even staggering of the charge radii in chains of isotopes of various elements as well as the explanation of the unusually large cross sections of two-nucleon and α-particle transfer reactions and the reduced widths of α decay, especially in the region of magic nuclei. The presence of the new phase discussed above can explain the existence of the experimentally observed superfluid isomers in ^{152}Sm.

A new type of first-order phase transition, i.e., a transition between the superfluid pairing phase and the new conjectured α-like phase can be found by studying two-nucleon transfer reactions in the region of Sm.

In conclusion, we note that the problem of nucleon correlations in superfluid nuclei is, on the one hand, a modern problem and well developed but, on the other hand, poorly understood. The solution of this problem will be the key to the description of cluster phenomena such as α decay,[19–25] the radioactivity of heavy particles,[26] and fission.

It is possible that a step forward was taken in a paper of Barranco *et al.*,[27] who, on the basis of a theory of collective motion with large amplitudes in superfluid nuclei, calculated for the first time effective factors for α, C, Ne, Mg, and Si decays. The agreement with the experimental data on decay with emission of heavy clusters is very good but it is rather poor for α decay. Of course, this conclusion indicates that α decay is mainly a collective phenomenon; however, the noncollective ingredients stimulate selection rules, which may change the collective picture.[19–25]

1. WHAT IS AN α CLUSTER?

The starting point for this discussion could be to check the definition of the word *cluster*, as it is given in several dictionaries.

A cluster is a group of identical or similar elements collected together or situated near each other. It is clear that this definition is so general that it becomes difficult to find examples of physical systems that do not consist of ensembles of clusters; moreover, today's cluster is yesterday's elementary particle. Bearing this in mind, perhaps it would be better to change the question and ask: What is not a cluster?

A system close to satisfying this definition may be one of the hither to unobse entities—a quark–gluon plasma.

The Bloch–Brink α-cluster model[28] includes variational calculations that use a trial wave function in which α clusters are regarded as elementary building blocks. The total energy of the system is minimized by the variation of parameters that are actually the centers of the α clusters. The model presupposes that α clusters are objects well localized in geometrical space and formed from two protons and two neutrons. The extensive and complicated investigations in the cluster model[29–35] include the multiconfiguration resonating-group method (RGM), the generator coordinate method (GCM), and the orthogonal condition method (OCM), proposed by the group of Wildermuth and Tang, Mikhaĭlovich's group, and a Japanese school. However, there also exist other types of cluster.

The strongest nucleon correlations in nuclei—pairing correlations—presuppose the existence, in a nucleus, of clusters constructed from correlated pairs of nucleons, although such clusters do not exist as free formations. Nevertheless, a good description of the spectra of 0^+ states and the strength of transitions between them can be obtained for nuclei near closed shells on the basis of a model that assumes the existence of elementary building blocks in the form of nucleon pairs with spin 0: the pair vibration model (PVM) of Bohr and Mottelson.[2]

A more general model that has a certain analogy with the PVM includes pairs with spin 0 and 2 and an interaction between them—the interacting boson model. This model describes reliably the pattern of energy levels and the transition strengths in a wide range of even–even nuclei even though the structure of the elementary bosons is not defined and they probably do not exist in the free state.

Although the clusters that are the building blocks in the PVM and IBM do not exist in the free state, they can be constructed in the framework of these models. In particular, both models can be used[36,37] to construct α-cluster states from pairs of neutrons and protons. This approach has success in explaining the observed picture of the α-particle transfer reaction more than in the case of two-particle transfer. Something that is not discussed in any of

these approaches is the question of the absolute strength of α transfers or the α-decay widths.

In the case of the α decay of heavy nuclei, the observed α-decay rates in general presuppose a relatively small percentage admixture of the decaying state [if it is described by shell-model wave functions with a residual (pairing +quadrupole) interaction] in the state of the daughter nucleus + α particle (if one works in the R-matrix formalism[25,38]). Theoretical estimates[19,25] of these quantities are in excellent agreement with the experimental data.

For light nuclei, the situation is somewhat better; namely, the α-cluster models can describe the transition rates, the absolute strengths of the α transitions, and the decay widths.[39] This is the case when the α-cluster structure is dominant in the structure of the nuclear states. There exist situations, indeed many of them, in which α clusters are not dominant in the structure of the nuclear states. This is the case for the low-lying 2^+ states in the ^{16}O nucleus, the structure of which is determined by many four-particle components distributed in the shells $1p_{1/2}$, $1d_{5/2}$, and $2s_{1/2}$ but not necessarily of two-proton and two-neutron type.

The Fermi liquid model was recently proposed[20] and tested[21–24] for various α transitions. This model appeared as a result of comprehensive analysis[19] of widely used models of α decay, and it was shown that the wave functions of the well-known modern models of nuclear structure are inadequate to describe α clustering, α decay, and α-transfer reactions. A nonpotential form of the scattering amplitude of the α-transition operator is needed. In the Fermi liquid a four-nucleon interaction for the irreducible amplitude of the α-cluster formation reaction in the four-particle channel is introduced into the α decay and α clustering on the basis of an idea of Migdal,[40] which follows from Landau's theory of quantum liquids. In this way, we can take into account the mismatch of the angular momenta. This Fermi liquid model for α clustering could be a first guess in the description of the phase transition from the Fermi-liquid state to the α-cluster state.

This picture of cluster states in nuclei makes it possible to identify quasistable states that have an origin based on complex cluster configurations. One of the best examples is ^{24}Mg, in which we find a diversity of cluster configurations having a large overlap with two ^{12}C nuclei, either in the ground state or in an excited 0^+ state. Indeed, once a statistical cluster configuration has been identified, it is possible to study the dynamics of this configuration, and then the identification of vibrational excitations coupled to the rotational degree of freedom has great complexities of the type observed in resonance scattering or $^{12}C+^{12}C$ reactions.

In recent years, there have been discoveries of a great diversity of cluster configurations, for example, fissioning shape isomers, superdeformed nuclei, etc. In Refs. 15–18, we introduced a special form of neutron–proton interaction which leads to a new type of correlation between protons and neutrons somewhat stronger than pairing correlations—dynamic α correlations. This type of correlation can be understood as intermediate between pairing correlations (for which the Cooper pair is regarded as a two-nucleon condensate) and an α condensate. One can say that we have proposed a new type of cluster constructed from two Cooper pairs (one proton pair and one neutron pair), but the interaction between these Cooper pairs is weaker than the interaction between the nucleons within a Cooper pair or an α condensate.

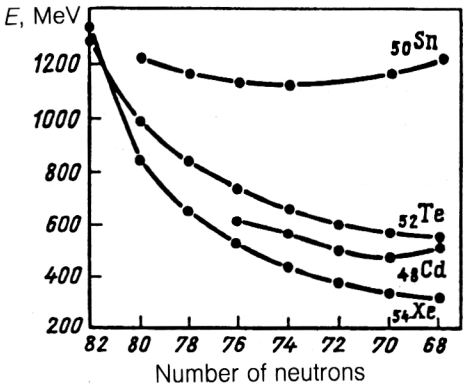

FIG. 1. Energies of the first 2^+ excited states as functions of the number of neutrons for singly magic tin nuclei and for neighboring elements with several valence protons.

2. SOME EXPERIMENTAL DATA RELATING TO THE PROTON–NEUTRON RESIDUAL INTERACTION IN NUCLEI

In what follows, we present some experimental data having a bearing on the introduction of a neutron–proton residual interaction in the average nuclear field.

Energy of 2^+ levels in magic nuclei

The energies of low-lying levels of even–even nuclei provide one of the examples of direct experimental data indicating the importance of the neutron–proton residual interaction. The energies of the lowest 2_1^+ excited states of nuclei in the region of Sn are shown in Fig. 1. They are almost equal for the Sn isotopes and much smaller for nonmagic nuclei. Since the energies of these lowest 2_1^+ excited states are typical for a collective state and deformation, the key role of the proton–neutron interactions is obvious—the valence proton–neutron residual interaction undoubtedly vanishes for Sn but not for other nuclei. It has been shown[41,42] that the excitation energies of j^n configurations are independent of n in the seniority scheme. Moreover, seniority is a good quantum number for many realistic two-nucleon residual interactions, for example, a δ-function interaction, acting on these configurations. Therefore, the constancy of the energies of the lowest 2_1^+ excited states for the Sn isotopes is not remarkable. An interesting feature of Fig. 1 is the very different behavior for nuclei near Sn with valence protons and neutrons. The proton–neutron residual interactions are much more effective when there is a simple nucleon configuration mixed[41] in the proton–neutron system than in states with $T=1$, which break the seniority scheme and eliminate the constancy of the excitation energies. Finally, the empirical be-

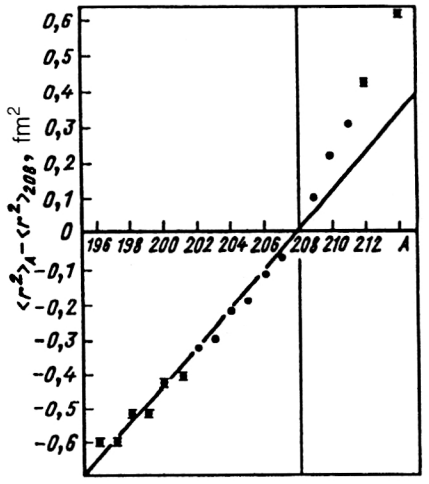

FIG. 2. Difference of the mean-square charge radius of Pb isotopes from calculations in the droplet model (sloping line).

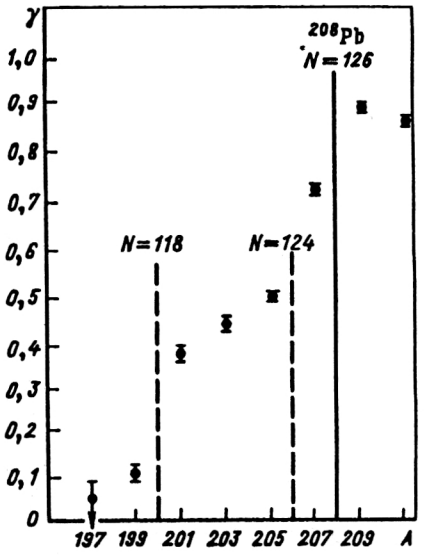

FIG. 3. Staggering parameter for Pb isotopes.

havior in Fig. 1 will be regarded as a basis for taking into account the role of proton–neutron residual interactions.

Odd–even staggerings of the charge radii of nuclei in chains of isotopes of various elements

The experimental data[7–11] on the isotopic shifts reveal a remarkable feature—characteristic "odd–even staggerings" of the charge radii in chains of isotopes of various elements. The staggerings reflect the fact that the mean square radii of the nuclei of odd-neutron isotopes are somewhat smaller (usually of the order of 10^{-2} fm^2) than the radii of the even-neutron neighboring nuclei (Fig. 2). With a few exceptions such behavior is observed in the entire periodic table and is confirmed with increasing accuracy. In some regions, for example, in highly neutron-deficient isotopes of Hg, Au, Sm, and Ce, the staggerings are very large and can be ascribed to special deformation effects.[43] In some other regions, for example, the lead and tin isotopes, specific shell effects are manifested.[44] However, apart from these special cases it is found that the charge radii of odd-neutron isotopes are smaller than the mean-square radii of the even-neutron neighboring nuclei. This effect is usually called the "normal odd–even staggering."

The isotope shifts are related to the nuclear parameters ($\lambda_{AA'}$) as follows:

$$\delta\nu_{AA'}=M\frac{A-A'}{AA'}+F\lambda_{AA'}, \tag{1}$$

where

$$\lambda=\delta\langle r^2\rangle+C_2\delta\langle r^4\rangle+C_3\delta\langle r^6\rangle+\ldots=0.93\delta\langle r^2\rangle \tag{2}$$

and

$$\delta\langle r^2\rangle_{AA'}=\langle r^2\rangle_A-\langle r^2_{A'}\rangle. \tag{3}$$

In Eq. (1),

$$F=22.1(3.3)\ \text{GHz/fm}^2, \tag{4}$$

$$M=7.1(13.1)\times NMS, \tag{5}$$

where NMS is the normal mass shift, equal to 27(270) MHz. The quantities F and M are determined by King's curve, which uses independent information on λ from a combined analysis of electron scattering and data on the muonic decay of stable isotopes.[11]

Another observable quantity associated with the staggerings is the staggering parameter

$$\gamma=\frac{2(\langle r^2\rangle_{A+1}-\langle r^2\rangle_A)}{\langle r^2\rangle_{A+2}-\langle r^2\rangle_A}$$

$$=\frac{2[\delta\nu_{A+1}-\delta\nu_A-M/A(A+1)]}{\delta\nu_{A+2}-\delta\nu_A-2M/A(A+2)}, \tag{6}$$

where A is an even–even nucleus. This staggering parameter can be extracted from the F factor, but with a reasonable estimate for M. For this quantity, Thompson *et al.*[10] proposed

$$M=1(10)\times NMS. \tag{7}$$

Recently, King and Wilson[45] deduced from theoretical calculations of the specific mass shifts in atomic transitions that

$$M=0.19(0.25)\times NMS. \tag{8}$$

The experimental staggering parameter[11] is always less than 1 and approaches 1 for magic numbers (Fig. 3); this is an experimental confirmation of the dominant part played by the residual proton–neutron interactions in this case.

Separation energies of unpaired nucleons

Figure 4 gives experimental separation energies of unpaired nucleons.[52] It can be seen that the separation energy of such nucleons increases with the addition of nucleons of the other species, and decreases with the addition of nucleons of the same species. Therefore (see, for example, Fig. 4a), $S(n)$ increases with increasing number of protons

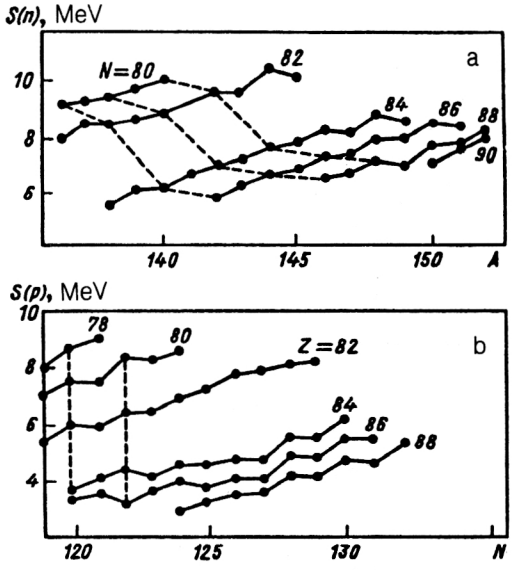

FIG. 4. Single-particle neutron (a) and proton (b) separation energies.

but decreases with increasing number of neutrons, i.e., in adding neutrons to the nucleus we make the last neutron less bound, whereas in adding protons we make the last neutron more bound. This is a simple and clear manifestation of the fact that on the average the interaction of like nucleons must be repulsive while that of unlike nucleons (proton–neutron interaction) must be attractive. Of course, this assertion applies to the component with zero isospin since the component with isospin, 1 must be identical in the proton–proton and neutron–neutron interactions. Therefore, the correlations are mainly due to the proton–neutron residual interaction.

Alpha decay of Pb isotopes

Alpha decay between ground states of even–even nuclei is favored.[19,25] The reduced widths for these s-wave transitions behave regularly as functions of the number of neutrons and the atomic number. They are greatest for α-decaying nuclei with two or four particles outside a closed shell (with an abrupt minimum at the shell) and decrease as the next closed shell is approached. It is known that most α-decaying heavy nuclei are superfluid and that a large part of the formation probability (the so-called spectroscopic factor) is due to pairing correlations.[3,19,25] The reduced widths for singly magic nuclei predicted by the pairing model is an order of magnitude smaller than for other α-decay nuclei and does not agree with experiment. However, the pairing model[3,53] does not contain residual proton–neutron interactions.

In a recent study Toth *et al.*[46] demonstrated experimentally that the reduced α-decay widths of neutron-deficient Pb isotopes have the same order as the superfluid nuclei in the region of the actinides and other nuclei that are neighbors of the Pb isotopes (Fig. 5).

This is a new experimental fact that must be regarded as confirming the role that can be played by residual proton–neutron interactions in describing, for example, the α decay of singly magic nuclei.

Single-particle energy levels in nuclei with one valence nucleon

In the multipole expansion of the residual effective proton–neutron interaction the monopole and quadrupole components are usually dominant. These two components give additional effects. It has been shown[47] that the monopole proton–neutron residual interaction shifts the single-particle energy levels of one particle species as a function of the number of nucleons of the other species. This occurs mainly because the order of the single-particle levels in the shell model is not the same through the complete chain of nuclei. A particularly dramatic example of such a situation is shown in Fig. 6, in which we compare the single-particle energies of ^{91}Zr, ^{131}Sn, and ^{207}Tl. The most striking change is the rapid decay of the $1g_{7/2}$ orbital from ^{91}Zr to ^{131}Sn.

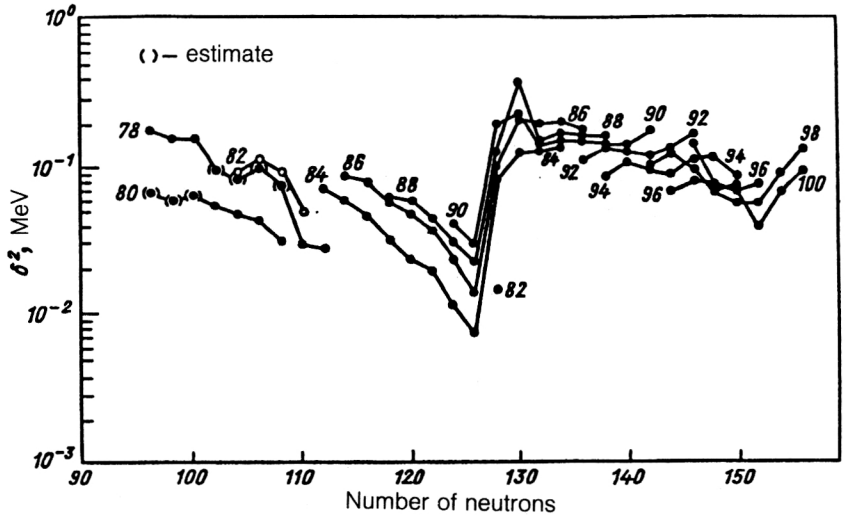

FIG. 5. Experimental reduced widths for s-wave α transitions as functions of the number of neutrons for isotopes with Z from 78 to 100.

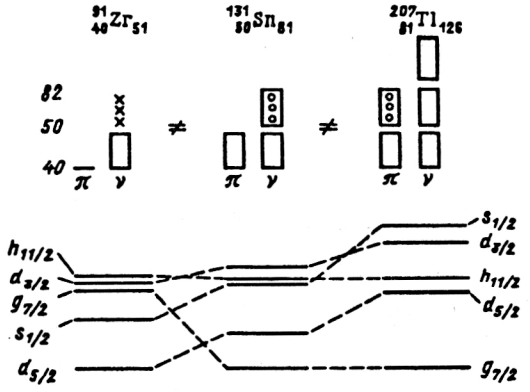

FIG. 6. Single-particle energy levels in nuclei with one valence nucleon. The rectangles above each level indicate the extent to which the levels are filled in each nucleus.

Between these two elements, with Z equal to 40 and 50, respectively, the proton orbital $1g_{7/2}$ is closed. The monopole interaction remains constant in the entire space, and, therefore, the proton–neutron matrix elements depend only on the overlap of the proton and neutron wave functions and will be greatest for similar orbitals. The attractive $p1g_{9/2}$–$n1g_{7/2}$ interaction from Zr to Sn leads to a decrease of these single-particle energies, as can be seen in Fig. 6. On the approach to Tl, the following, higher neutron and proton shells are filled, and they have, on the average, higher values of j than for the lower shells. Therefore, there tends to be an increase in the attractive interaction for orbitals filled higher in j than lower in j. This effect is also demonstrated in Fig. 6, in which the orbitals with higher j are situated below the single-particle levels with lower j.

3. ENLARGED SUPERFLUID MODEL

The Hamiltonian

The enlarged superfluid model for nonrotational states of deformed nuclei includes the average field of the neutron and proton systems in the form of the axisymmetric Woods–Saxon (or Hartree–Fock) potential, monopole pairing, isoscalar and isovector *ph* and *pp* multipole and spin-multipole interactions between quasiparticles, and the so-called α-like four-nucleon interaction.[15–18] For the *ph* and *pp* multipole and spin-multipole interactions, we use a separable interaction[48–51] of rank $N>1$:

$$H=H_0+H', \tag{9}$$

where

$$H_0=\sum_{\tau}(H^{\rm av}_{\rm s.p}(\tau)-G_\tau P^\dagger_\tau P_\tau)+H_4, \tag{10}$$

in which

$$H^{\rm av}_{\rm s.p}(\tau)=\sum_{s\sigma}E_s a^\dagger_{s\sigma}a_{s\sigma}, \tag{11}$$

$$P_\tau=\sum_s a_{s-}a_{s+}, \tag{12}$$

$$H_4=G_4P^\dagger_pP^\dagger_nP_nP_p \tag{13}$$

and

$$\begin{aligned}H'=\sum_\tau\Bigg\{&-\frac{1}{2}\sum_{\lambda\mu\sigma}\sum_{n=1}^{N}\Bigg[\sum_{\eta=\pm1}(k^{\lambda\mu}_{0\tau}\\&+\eta k^{\lambda\mu}_{1\tau})Q^\dagger_{n\lambda\mu\sigma}(\tau)Q_{n\lambda\mu\sigma}(\eta\tau)\\&+G^{\lambda\mu}_\tau P^\dagger_{n\lambda\mu\sigma}(\tau)P_{n\lambda\mu\sigma}(\tau)\Bigg]\\&-\frac{1}{2}\sum_{L\lambda\mu\sigma}\sum_{n=\pm1}^{N}\Bigg[\sum_{\eta=\pm1}(k^{L\lambda\mu}_{0\tau}\\&+\eta k^{L\lambda\mu}_{1\tau})T^\dagger_{nL\lambda\mu\sigma}(\tau)T_{nL\lambda\mu\sigma}(\eta\tau)\\&+G^{L\lambda\mu}_\tau P^\dagger_{nL\lambda\mu\sigma}(\tau)P_{nL\lambda\mu\sigma}(\tau)\Bigg]\Bigg\}.\end{aligned} \tag{14}$$

Here, $\tau=\pm1/2$ for the protons and neutrons, respectively, $a^\dagger_{s_\tau\sigma_\tau}$ ($a_{s_\tau\sigma_\tau}$) are the fermion operators of creation (annihilation) of nucleons in the single-particle state $|s_\tau\sigma_\tau\rangle$, where σ_τ is the symbol of projection of the angular momentum of the state onto the symmetry axis of the nucleus, and s_τ denotes the remaining (N_τ, n_{Z_τ}, Ω_τ, π_τ...) quantum numbers that identify the single-particle energy levels. The term H_4 in Eq. (13) is the effective coherent interaction of two pairs (four nucleons), including dynamical α-type correlations of four nucleons in the superfluid nuclear phase.[15–18] The strength of the pairing interaction is given by G_τ, and $G^{\lambda\mu}_\tau$ and $G^{L\lambda\mu}_\tau$ are the coupling constants of the *pp* interaction;[15] $k^{\lambda\mu}_{0\tau}$, $k^{\lambda\mu}_{1\tau}$ and $k^{L\lambda\mu}_{0\tau}$, $k^{L\lambda\mu}_{1\tau}$ are the isoscalar and isovector coupling constants of the *ph* multipole–multipole and spin-multipole interactions;[3] G_4 is the constant of the four-nucleon interaction, and $\sigma=\pm1$. We make a Bogolyubov–Valatin canonical transformation

$$a_{s\sigma}=u_s\alpha_{s-\sigma}+\sigma v_s\alpha^\dagger_{s\sigma} \tag{15}$$

and obtain

$$P_\tau=\sum_s\left[u_sv_s+\frac{1}{2\sqrt{2}}A^{(+)}_{(-)}(ss)-\frac{1}{2\sqrt{2}}v^{(-)}_{ss}A^{(+)}_{(-)}(ss)-\frac{1}{2}u^{(+)}_{ss}B_{(+)}(ss)\right], \tag{16}$$

$$P_{n\lambda\mu\sigma} \text{ or } P_{nL\lambda\mu\sigma}=\sum_{ss'}\Big[\delta_{ss'}p^{(-)}_{ss'}u_s v_s-\frac{1}{2\sqrt{2}}p^{(+)}_{ss'}[v^{(-)}_{ss'}\overline{A}^{(+)}_{(+)}(ss')+v^{(+)}_{ss'}\overline{A}^{(-)}_{(+)}(ss')]+\frac{1}{2\sqrt{2}}p^{(-)}_{ss'}[v^{(+)}_{ss'}\overline{A}^{(+)}_{(-)}(ss')$$
$$+v^{(-)}_{ss'}\overline{A}^{(-)}_{(-)}(ss')]-\frac{1}{2\sqrt{2}}\bar{p}^{(+)}_{ss'}[v^{(+)}_{ss'}A^{(+)}_{(+)}(ss')+v^{(-)}_{ss'}A^{(-)}_{(+)}(ss')]$$
$$-\frac{1}{2\sqrt{2}}\bar{p}^{(-)}_{ss'}[v^{(-)}_{ss'}A^{(+)}_{(-)}(ss')+v^{(+)}_{ss'}A^{(-)}_{(-)}(ss')]+\frac{1}{4}p^{(-)}_{ss'}[u^{(-)}_{ss'}\overline{B}^{(-)}_{(+)}(ss')+u^{(+)}_{ss'}\overline{B}^{(-)}_{(+)}(ss')]$$
$$+\frac{1}{4}p^{(+)}_{ss'}[u^{(-)}_{ss'}\overline{B}^{(-)}_{(-)}(ss')+u^{(+)}_{ss'}\overline{B}^{(+)}_{(-)}(ss')]-\frac{1}{4}\bar{p}^{(-)}_{ss'}[u^{(+)}_{ss'}B^{(+)}_{(+)}(ss')+u^{(-)}_{ss'}B^{(-)}_{(+)}(ss')]$$
$$+\frac{1}{4}\bar{p}^{(+)}_{ss'}[u^{(-)}_{ss'}B^{(+)}_{(-)}(ss')+u^{(+)}_{ss'}B^{(-)}_{(-)}(ss')]\Big], \tag{17}$$

$$Q_{n\lambda\mu\sigma} \text{ or } T_{nL\lambda\mu\sigma}=\sum_{ss'}\Big[\delta_{ss'}v_s^2 q^{(+)}_s+\frac{1}{2\sqrt{2}}q^{(+)}_{ss'}[u^{(+)}_{ss'}A^{(+)}_{(-)}(ss')+u^{(-)}_{ss'}A^{(-)}_{(-)}(ss')]-\frac{1}{2\sqrt{2}}q^{(-)}_{ss'}[u^{(-)}_{ss'}A^{(+)}_{(+)}(ss')$$
$$+u^{(+)}_{ss'}A^{(-)}_{(+)}(ss')]-\frac{1}{2\sqrt{2}}\bar{q}^{(+)}_{ss'}[u^{(-)}_{ss'}\overline{A}^{(+)}_{(-)}(ss')+u^{(+)}_{ss'}\overline{A}^{(+)}_{(-)}(ss')]$$
$$+\frac{1}{2\sqrt{2}}\bar{q}^{(-)}_{ss'}[u^{(+)}_{ss'}\overline{A}^{(+)}_{(+)}(ss')+u^{(-)}_{ss'}\overline{A}^{(-)}_{(+)}(ss')]+\frac{1}{4}q^{(+)}_{ss'}[v^{(-)}_{ss}B^{(+)}_{(+)}(ss')+v^{(+)}_{ss'}B^{(-)}_{(+)}(ss')]$$
$$-\frac{1}{4}q^{(-)ss'}[v^{(-)}_{ss'}B^{(-)}_{(-)}(ss')-v^{(+)}_{ss'}B^{(+)}_{(-)}(ss')]+\frac{1}{4}\bar{q}^{(+)}_{ss'}[v^{(+)}_{ss'}\overline{B}^{(+)}_{(+)}(ss')$$
$$+v^{(-)}_{ss'}\overline{B}^{(-)}_{(+)}(ss')]-\frac{1}{4}\bar{q}^{(-)}_{ss'}[v^{(-)}_{ss'}\overline{B}^{(+)}_{(-)}(ss')+v^{(+)}_{ss'}\overline{B}^{(-)}_{(-)}(ss')]\Big], \tag{18}$$

where

$$A^{(\pm)}_{(+)}(ss')=A^{\dagger}_{(+)}(ss')\pm A_{(+)}(ss'),\quad A^{\pm}_{(-)}(ss')=A^{\dagger}_{(-)}(ss')\pm A_{(-)}(ss'),$$
$$\overline{A}^{\pm}_{(+)}(ss')=\overline{A}^{\dagger}_{(+)}(ss')\pm\overline{A}_{(+)}(ss'),\quad \overline{A}^{\pm}_{(-)}(ss')=\overline{A}^{\dagger}_{(-)}(ss')\pm\overline{A}_{(-)}(ss'),$$
$$B^{\pm}_{(+)}(ss')=B^{\dagger}_{(+)}(ss')\pm B_{(+)}(ss'),\quad B^{\pm}_{(-)}(ss')=B^{\dagger}_{(-)}(ss')\pm B_{(-)}(ss'),$$
$$\overline{B}^{\pm}_{(+)}(ss')=\overline{B}^{\dagger}_{(+)}(ss')\pm\overline{B}_{(+)}(ss'),\quad \overline{B}^{\pm}_{(-)}(ss')=\overline{B}^{\dagger}_{(-)}(ss')\pm\overline{B}_{(-)}(ss'),$$
$$A_{(+)}(ss')=\frac{1}{\sqrt{2}}\sum_{\sigma}\alpha_{s\sigma}\alpha_{s'-\sigma},\quad A_{(-)}(ss')=\frac{1}{\sqrt{2}}\sum_{\sigma}\sigma\alpha_{s\sigma}\alpha_{s'-\sigma},\quad \overline{A}_{(+)}(ss')=\frac{1}{\sqrt{2}}\sum_{\sigma}\alpha_{s\sigma}\alpha_{s'\sigma}, \tag{19}$$
$$\overline{A}_{(-)}(ss')=\frac{1}{\sqrt{2}}\sum_{\sigma}\sigma\alpha_{s\sigma}\alpha_{s'\sigma},\quad B_{(+)}(ss')=\sum_{\sigma}\alpha^{\dagger}_{s\sigma}\alpha_{s'\sigma},\quad B_{(-)}(ss')=\sum_{\sigma}\sigma\alpha^{\dagger}_{s\sigma}\alpha_{s'\sigma},$$
$$\overline{B}_{(+)}(ss')=\sum_{\sigma}\alpha^{\dagger}_{s-\sigma}\alpha_{s'\sigma},\quad \overline{B}_{(-)}(ss')=\sum_{\sigma}\sigma\alpha^{\dagger}_{s-\sigma}\alpha_{s'},$$

and

$$p^{\pm}_{ss'}=p_{++}(ss')\pm p_{--}(ss'),\quad \bar{p}^{\pm}_{ss'}=p_{+-}(ss')\pm p_{-+}(ss'),\quad q^{\pm}_{ss'}=q_{++}(ss')\pm q_{--}(ss'),$$
$$\bar{q}^{\pm}_{ss'}=q_{+-}(ss')\pm q_{-+}(ss'),\quad u^{\pm}_{ss'}=u_s v_{s'}\pm v_s u_{s'},\quad v^{\pm}_{ss'}=u_s u_{s'}\pm v_s v_{s'}. \tag{20}$$

The matrix elements of the *pp* and *ph* multipole and spin-multipole interactions are

$$p_{\sigma\sigma'}(ss')=\langle s\sigma|\hat{p}|s'\sigma'\rangle \tag{21}$$

$$q_{\sigma\sigma'}(ss')=\langle s\sigma|\hat{q}|s'\sigma'\rangle \tag{22}$$

with

$$\hat{p}=\mathscr{R}^{\lambda\mu}_{n(pp)}(r)\,Y_{\lambda,\sigma\mu}(\hat{r})$$

or

$$\hat{p}=\mathscr{R}^{L\lambda\mu}_{n(pp)}(r)\{\hat{\sigma}Y_L\}_{\lambda,\sigma\mu},$$
$$\hat{q}=\mathscr{R}^{\lambda\mu}_{n(ph)}(r)\,Y_{\lambda,\sigma\mu}(\hat{r}), \tag{23}$$

or

$$\hat{q}=\mathscr{R}^{L\lambda\mu}_{n(ph)}(r)\{\hat{\sigma}Y_L\}_{\lambda,\sigma\mu}. \tag{24}$$

The properties of the *pp* and *ph* matrix elements are discussed in Ref. 3.

Equations for the gap

As a trial wave function for the nuclear ground state we use a wave function of BCS type, and for a start we take only the H_0 part of the Hamiltonian (9):

$$|\mathrm{BCS}\rangle=\prod_{\tau s_\tau}(u_{s_\tau}+v_{s_\tau}a^\dagger_{s_\tau}+a^\dagger_{s_\tau-})|0\rangle, \tag{25}$$

where $u_s^2+v_s^2=1$ and $|0\rangle$ denotes the absolute vacuum.

Then the energy functional is

$$W=\langle\mathrm{BCS}|H_0-\sum_\tau\lambda_\tau\hat{N}_\tau|\mathrm{BCS}\rangle$$

$$=\sum_\tau\left(\sum_{s_\tau}2(\tilde{E}_{s_\tau}-\lambda_\tau)v^2_{s_\tau}-G_\tau\chi^2_\tau\right)-G_4\chi^2_p\chi^2_n. \tag{26}$$

Here, λ_τ is the Fermi level for a nucleon, $\hat{N}_\tau$ is the operator of the nucleon number,

$$\chi_\tau=\langle\mathrm{BCS}|\sum_{s_\tau}a^\dagger_{s_\tau}+a^\dagger_{s_\tau-}|\mathrm{BCS}\rangle+\sum_{s_\tau}u_{s_\tau}v_{s_\tau} \tag{27}$$

is the so-called pair correlation function or order parameter, and

$$\tilde{E}_{s_{\mathrm{p(n)}}}=E_{s_{\mathrm{p(n)}}}-\frac{1}{2}(G_{p(n)}+G_4\chi^2_{n(p)})v^2_{s_{\mathrm{p(n)}}}$$

$$-\frac{1}{4}G_4v^2_{s_{\mathrm{p(n)}}}\sum_{s_{\mathrm{n(p)}}}v^4_{s_{\mathrm{n(p)}}} \tag{28}$$

are modified (compared with $E_{s_{\mathrm{p(n)}}}$) single-particle energies. These corrections to the self-consistent field are usually omitted.[3]

Minimization of the function W with respect to the variational parameters given by Eq. (26) leads to the equations

$$\frac{1}{2}(G_{p(n)}+G_4\chi^2_{n(p)})\sum_{s_{\mathrm{p(n)}}}\varepsilon^{-1}_{s_{\mathrm{p(n)}}}=1,$$

$$\sum_{s_\tau}[1-(\tilde{E}_{s_\tau}-\lambda_\tau)\varepsilon^{-1}_{s_\tau}]=N_\tau, \tag{29}$$

$$\varepsilon_{s_\tau}=\sqrt{(\tilde{E}_{s_\tau}-\lambda_\tau)^2+\Delta^2_\tau},$$

for even–even deformed superfluid nuclei. For odd and odd–odd deformed superfluid nuclei, these equations are modified with allowance for the blocking effect.[3]

The Bogolyubov–Valatin parameters u_s and v_s are chosen in accordance with the formula

$$\begin{pmatrix}u^2_{s_\tau}\\ v^2_{s_\tau}\end{pmatrix}=\frac{1}{2}\left(1\pm\frac{\tilde{E}_{s_\tau}-\lambda_\tau}{\varepsilon_{s_\tau}}\right), \tag{30}$$

and the correlation function takes the form

$$\chi_\tau=\frac{1}{2}\Delta_\tau\sum_{s_\tau}\varepsilon^{-1}_{s_\tau}. \tag{31}$$

The equations for the initial gap and constraint with allowance for trivial solutions have the form

$$\Delta_{p(n)}=\chi_{p(n)}(G_{p(n)}+G_4\chi^2_{n(p)})\sum_{s_\tau}2v^2_{s_\tau}=N_\tau. \tag{32}$$

The trivial solutions $\Delta_\tau=0$ exist always, but there are cases when the total minimum of the correlation energy (which determines the ground state of the nucleus) is obtained for nontrivial solutions. These are the cases of superfluid nuclei.

The equations for the gap in spherical nuclei are obtained from the above equations for the gap by the simple replacement of ε_s^{-1} by $\Omega_s\varepsilon_s^{-1}$, whereas in the constraint equation we must multiply each term in the sum by $\Omega_s=\frac{1}{2}(2j_s+1)$. The correlation function is modified in accordance with the prescriptions of the equations for the gap.

A simple investigation of the equations for the gap shows that the proton and neutron equations are coupled, i.e., it is possible that the superfluidities of the proton and neutron systems generate each other even when the Belyaev condition[53] is not satisfied for one system in the absence of four-nucleon interactions. The additional term $G_4\chi^2$ can increase the pairing forces, bringing about fulfillment of the Belyaev condition. Moreover, as we shall see below, the equations for the gap can, for some nuclei, have more than one set of solutions, and this fact opens up a new field of investigations.

Determination of coupling constants from experiment

To determine the coupling constants in a number of studies in the framework of the ESM for special cases we use the well-known mass difference[3]

$$P_Z=\frac{1}{2}\{2\varepsilon(Z-1,N)-\varepsilon(Z,N)-\varepsilon(Z-2,N)\}, \tag{33}$$

$$P_N=\frac{1}{2}\{2\varepsilon(Z,N-1)-\varepsilon(Z,N)-\varepsilon(Z,N-2)\} \tag{34}$$

for the pairing interaction (G_p and G_n) and

$$P_4=\varepsilon(Z,N)-\varepsilon(Z-2,N-2)-\varepsilon(Z+1,N)$$

$$+\varepsilon(Z-1,N)-\varepsilon(Z,N+1)+\varepsilon(Z,N-1) \tag{35}$$

for the four-nucleon interaction (G_4).[18] Then

$$\varepsilon(Z,N)=\sum_\tau\left(\sum_{s_\tau}2E_{s_\tau}v^2_{s_\tau}-G_\tau\chi^2_\tau\right)-G_4\chi^2_p\chi^2_n \tag{36}$$

for an even–even nucleus, and

TABLE I. ESM coupling constants and parameters of the energy gap calculated with and without allowance for the H_4 interaction for various nuclei.

Nucleus	C_p	C_n	C_4	Δ_p, MeV	Δ_n, MeV
$^{152}_{60}Nd_{92}$	19,3	17,1	27,7	1,170	1,160
	26,4	23,6	0	0,920	1,110
$^{156}_{62}Sm_{94}$	18,3	18,0	29,2	0,777	0,889
	24,4	21,8	0	0,685	0,850
$^{160}_{64}Gd_{96}$	21,0	21,6	27,0	0,832	0,991
	26,7	24,9	0	0,752	0,925
$^{164}_{66}Dy_{98}$	24,2	21,8	22,7	0,818	0,833
	27,7	24,6	0	0,739	0,800
$^{168}_{68}Er_{100}$	25,5	22,1	27,6	0,949	0,887
	29,4	26,1	0	0,832	0,839
$^{176}_{72}Hf_{104}$	23,2	19,9	19,1	0,755	0,843
	27,8	22,3	0	0,737	0,840
$^{180}_{74}W_{106}$	26,8	19,8	22,2	0,908	0,803
	31,3	23,0	0	0,878	0,786
$^{184}_{76}Os_{108}$	24,1	25,2	22,1	0,688	1,175
	31,6	26,3	0	0,670	1,080
$^{240}_{94}Pu_{146}$	34,0	21,5	15,2	0,900	0,685
$^{246}_{98}Cf_{148}$	31,7	19,9	14,5	0,609	0,355

$$\varepsilon(Z-1,N)=E_{s_{0,p}}+\sum_{s_p\neq s_{0,p}}2E_{s_p}v_{s_p}^2+\sum_{s_n}2E_{s_n}v_{s_n}^2-G_p\tilde{\chi}_p^2$$
$$-G_n\chi_n^2-G_4\tilde{\chi}_p^2\chi_n^2 \qquad (37)$$

for an odd-proton nucleus,[3] where

$$\tilde{\chi}_p=\sum_{s_p\neq s_{0,p}}u_{s_p}v_{s_p}. \qquad (38)$$

The experimental values of P_Z, P_N, and P_4 are obtained from Eqs. (35)–(37) by replacement of the energies ε by the experimental binding energies $(-B)$.[54] We can choose P_4 by the same method by analogy with the quantity for pairing vibrations,[2,3,52] namely,

$$P_4\cong\varepsilon(Z,N)-\varepsilon(Z-2,N-2)-2\lambda_p-2\lambda_n. \qquad (39)$$

Eight nuclei are considered to determine P_Z, P_N, and P_4. For each nucleus of this set, we must solve a system of 35 nonlinear equations with 35 unknowns for each nucleus (Z,N). Taking into account in the usual manner the $A=(Z+N)$ dependence of the coupling constants

$$G_p=\frac{1}{A}C_p,\quad G_n=\frac{1}{A}C_n \qquad (40)$$

and

$$G_4=\frac{1}{A_2}C_4, \qquad (41)$$

TABLE II. Experimental odd-even mass differences and the value of P_4 [see Eq. (27)] calculated with and without allowance for the H_4 interaction for various nuclei.

Nucleus	P_Z, MeV (exp)	P_Z, MeV (theor)	P_N, MeV (exp)	P_N, MeV (theor)	P_4, MeV (exp)	P_4, MeV (theor)
$^{152}_{60}Nd_{92}$	0,675	0,676	0,971	0,973	0,163	0,104
		0,674		0,971		−0,736
$^{156}_{62}Sm_{94}$	0,474	0,474	0,721	0,721	−0,177	−0,181
		0,473		0,720		−0,617
$^{160}_{64}Gd_{96}$	0,517	0,517	0,754	0,752	−0,216	−0,218
		0,517		0,754		−0,766
$^{164}_{66}Dy_{98}$	0,428	0,429	0,684	0,684	−0,582	−0,576
		0,428		0,684		−0,825
$^{168}_{68}Er_{100}$	0,504	0,504	0,667	0,667	−0,401	−0,401
		0,504		0,667		−0,883
$^{176}_{72}Hf_{104}$	0,594	0,593	0,728	0,727	−0,348	−0,340
		0,593		0,728		−0,576
$^{180}_{74}W_{106}$	0,681	0,681	0,741	0,742	0,076	0,070
		0,680		0,741		−0,508
$^{184}_{76}Os_{108}$	0,439	0,440	0,910	0,912	−0,823	−0,830
		0,439		0,910		−1,222
$^{240}_{94}Pu_{146}$	0,591	0,603	0,443	0,419	−0,313	−0,326
$^{246}_{98}Cf_{148}$	0,538	0,542	0,546	0,543	−0,266	−0,253

TABLE III. Superfluid correlation functions [see Eq. (19)] (spectroscopic factors) calculated with and without allowance for the H_4 interaction for various nuclei.

Nucleus	C_4	χ_p^2	χ_n^2
$^{152}_{60}Nd_{92}$	27,7	37,7	53,6
	0	27,9	51,5
$^{156}_{62}Sm_{94}$	29,2	22,4	38,7
	0	19,1	37,5
$^{160}_{64}Gd_{96}$	27,0	23,4	38,3
	0	20,2	35,2
$^{164}_{66}Dy_{98}$	22,7	22,0	29,7
	0	19,0	28,2
$^{168}_{68}Er_{100}$	27,6	26,9	31,2
	0	22,2	29,2
$^{176}_{72}Hf_{104}$	19,1	22,3	44,0
	0	21,9	43,8
$^{180}_{74}W_{106}$	22,2	26,6	38,9
	0	25,4	37,7
$^{184}_{76}Os_{108}$	22,1	15,9	63,1
	0	15,2	56,9
$^{240}_{94}Pu_{146}$	15,2	33,7	47,6

we calculate for some nuclei in the region of the rare earths and actinides the gap parameters C_p, C_n, C_4 and the theoretical values of P_Z, P_N, P_4, which are chosen as close as possible to the experimental values. The results of Ref. 18 are given in Tables I–III and in Figs. 7–12. The expression (41) can be obtained by assuming approximate factorization of the vertex of the two-pair interaction with coupling forces in the form (40). We attempted to fit the experimental mass differences P_Z, P_N, P_4 on the basis of an A dependence of G_4 close to $1/A^2$ ($1/A^{5/3}$ or $1/A^{7/3}$), but the fit was unsuccessful. In the calculations, the energy cutoff includes approximately 40 neutron and 40 proton levels of the deformed Woods–Saxon potential.[55] The gap parameters are slightly increased in the region of superfluid nuclei, when G_4 comes into play. However, at the boundary of the superfluid regions we can have more than one solution, and, of course, the gap parameters have different behavior.

Solutions of the gap equations and the phase diagram

The boundary between the normal and superfluid nuclei when $G_4=0$ is given by[53]

$$G_{p(n)}=G_{p(n)}^{\mathrm{cr}}, \tag{42}$$

where

$$\frac{1}{2}G_\tau^{\mathrm{cr}}\sum_{s_\tau}\frac{\Omega_{s_\tau}}{|\tilde{E}_{s_\tau}-\lambda_\tau|}=1 \tag{43}$$

with $\Omega_s=1$ for a deformed axisymmetric nucleus and $\Omega=\frac{1}{2}(2j_s+1)$ for a spherical nucleus. The phase structure of this model with respect to the controllable parameters G_τ decreases (independently of the neutrons and protons) the normal phases for $G_\tau\leqslant G_\tau^{\mathrm{cr}}$ and the superfluid phases otherwise, and the phase transitions are of second order. Such phase transitions are observed in two-nucleon transfer reactions,[56] in α-clustering processes, etc. In the case of our model, an analogous boundary is not observed. A complete discussion covering the three controllable parameters (G_p, G_n, G_4) and an arbitrary single-particle spectrum is practically impossible. To understand the nature of the phase structure and identify the specific features associated with the strength G_4 of the new interaction, we discuss a simplified model that warrants attention in its own right and has very nontrivial behavior in a realistic case.

We assume that the single-particle part (10) of the Hamiltonian (9) has equidistant spectrum for two fermion species (we shall call this simplified single-particle model the homogeneous model), and introduce the notation

$$\tilde{E}_{s_\tau}=E_F(\tau)-k/\rho_\tau, \tag{44}$$

$$\lambda_\tau=E_F(\tau)+\sigma_\tau/\rho_\tau, \tag{45}$$

$$g_\tau=\rho_\tau G_\tau, \tag{46}$$

$$x_\tau=(\rho_\tau\Delta_\tau)^2, \tag{47}$$

$$g_4=\rho G_4, \tag{48}$$

where

$$\rho=\frac{1}{2}(\rho_p+\rho_n) \tag{49}$$

and k are integers belonging to the Λ shells[57] (energy cutoff) and are determined by the intervals $[-N_{1,\tau}, N_{2,\tau}]$; $E_F(\tau)$ and λ_τ are, respectively, the Fermi energies for noninteracting fermions by means of $H_{\mathrm{pair}}+H_4$ and for interacting fermions by means of $H_{\mathrm{pair}}+H_4$ of the type τ. Moreover, we analyze the "symmetric" case, when the protons and neutrons have identical properties,

$$\begin{aligned}&\rho_p=\rho_n=\rho, \quad g_p=g_n=g_2,\\ &\lambda_p=\lambda_N=\lambda, \quad \sigma_p=\sigma_n=\sigma,\end{aligned} \tag{50}$$

and for which the gap equations have only symmetric solutions

$$x=x_p=x_n, \tag{51}$$

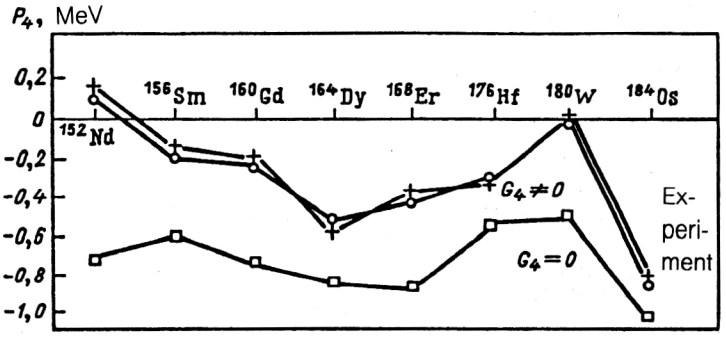

FIG. 7. Experimental and theoretical values of P_4 (with and without allowance for H_4) [see Eq. (27) and the text].

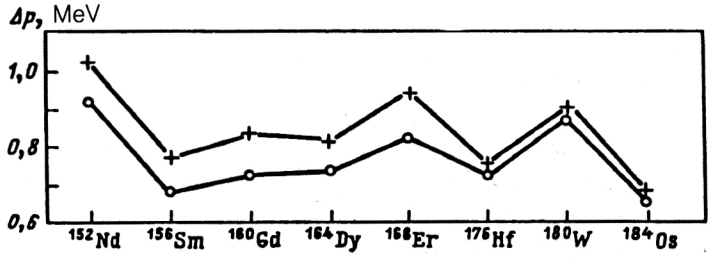

FIG. 8. Proton pairing energy gap (with and without allowance for the H_4 interaction).

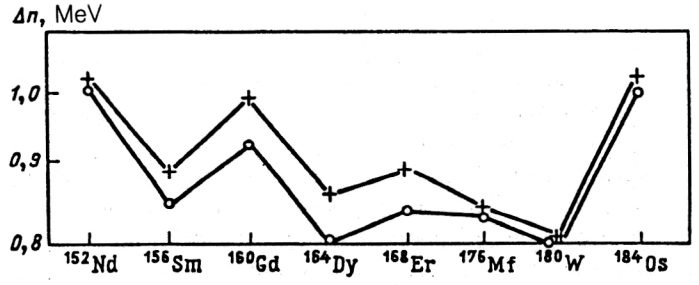

FIG. 9. Neutron pairing energy gap (with and without allowance for the H_4 interaction).

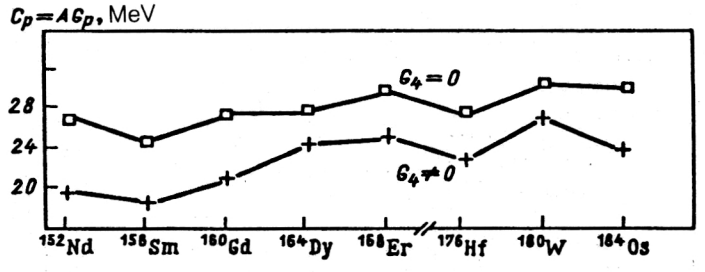

FIG. 10. Proton pairing constant.

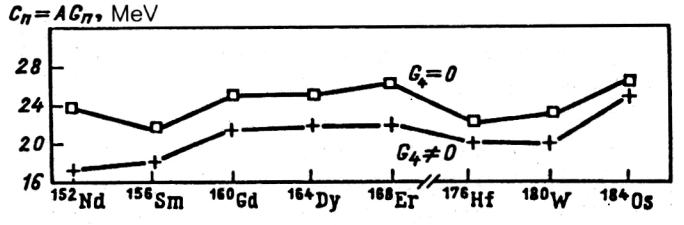

FIG. 11. Neutron pairing constant.

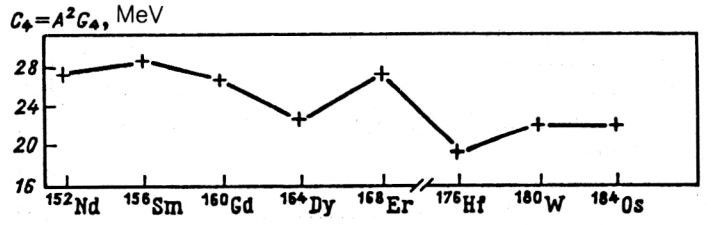

FIG. 12. Constant of the four-nucleon interaction.

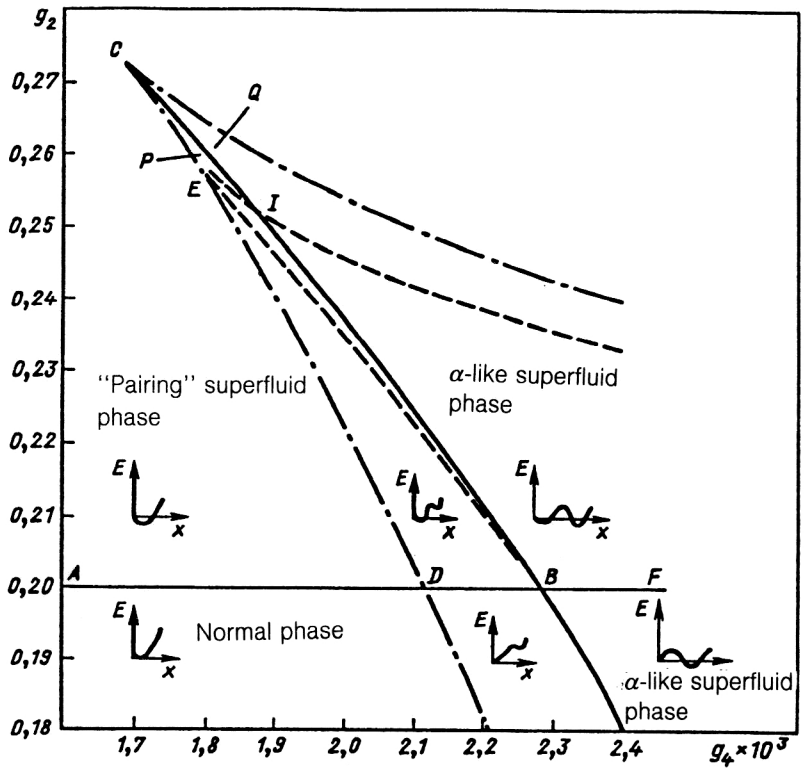

FIG. 13. Phase diagram.

and in the case of a half-filled Λ shell

$$N_{1,\tau}=n, \quad N_{2,\tau}=n+1 \tag{52}$$

the constraint equation in (29) has the solution

$$\sigma_\tau=\sigma=1/2. \tag{53}$$

The correlation energy in our model becomes

$$\begin{aligned}\varepsilon=\rho E_{\text{corr}}&=\rho[W(x)-W(0)]\\&=2(n+1)^2-4S_1(x)+4xS_{-1}(x)\\&\quad-2g_2xS^2_{-1}(x)-g_4x^2S^4_{-1}(x)\end{aligned} \tag{54}$$

with

$$S_j(x)=\frac{1}{2}\sum_{k=-n}^{n+1}\left[x+\left(k-\frac{1}{2}\right)^2\right]^{j/2}, \tag{55}$$

which must be studied for the solution of the gap equation

$$F(x)=[g_2+g_4xS^2_{-1}(x)]S_{-1}(x)-1=0. \tag{56}$$

To find the number and nature of solutions of Eq. (56), it will be helpful to use the following curves in the (g_2, g_4):

$$F(x)=0, \quad \frac{dF(x)}{dx}=0, \tag{57}$$

$$\varepsilon(0)=0, \quad F(0)=0, \tag{58}$$

$$\varepsilon(x_1)=\varepsilon(x_3)<0 \tag{59}$$

and, additionally,

$$\varepsilon(x)=0, \quad F(x)=0. \tag{60}$$

For $n=20$, the curve (57) (chain curve in Fig. 13) separates regions in which the numbers of solutions of the gap equation (56) differ by a factor two. The curve (56) [continuous and horizontal *(ADBF)*, beginning at the point $(g_2=0.2, g_4=0)$] separates regions in which the numbers of solutions differ by 1 and in the case $g_4=0$ decreases the critical value obtained from the Belyaev condition.[53] At the point of intersection of the curve (59) (continuous curve *CIBH* in Fig. 13), the system changes its global minimum from $\varepsilon(x_1)$ to $\varepsilon(x_3)$, where the solution x_2 corresponds to the maximum of the correlation energy $\varepsilon(x)$. Intersection of the curve (60) (broken curve in Fig. 13) changes the sign of the correlation energy for one solution of the gap equation (56). It must also be borne in mind that the global minimum of the correlation energy (54) corresponds to the ground state of the system, whereas a local minimum can describe a metastable state. Bearing in mind that the derivatives of the correlation energy (54) with respect to the controllable parameters g_2 and g_4 for $x=x_0$, where x_0 is a solution of the gap equation (56),

$$\frac{d\varepsilon(x)}{dg_2}=-2x_0S^2_{-1}(x_0)<0, \tag{61}$$

$$\frac{d\varepsilon(x)}{dg_4}=-x_0^2S^4_{-1}(x_0)<0, \tag{62}$$

jump when the gap parameter has a discontinuity, we arrive at the following conclusions (see Fig. 13).

If for the moment we forget the trivial solutions of the gap equation ($\Delta_p=0$ and $\Delta_n=0$) in the region *OADG*, then Eq. (56) has no solutions, and the ground state of the system exists in the normal phase.

In the region *ADECF*, the gap equation has one solution, which corresponds to a negative minimum of the cor-

relation energy. The ground state of the system is in the pairing superfluid phase.[15–18]

In the region *GDECFHG*, the gap equation has three solutions, two of which correspond to a minimum of the correlation energy, and one to a maximum. One of the minima is deeper (global minimum) and corresponds to the ground state of the system; the other (local minimum) corresponds to a metastable state. If this metastable state has a long lifetime, it can be regarded as an isomer. In the region *HBDC*, the ground state is in the normal phase, whereas the metastable state corresponding to a local minimum is in an α-like superfluid phase.[15–18]

In the region *BDC*, the ground state is in the pairing superfluid phase, while the metastable state is in the α-like superfluid phase.

In the region *BCF*, the situation is reversed—the ground state is in the α-like superfluid phase, and the metastable state is in the pairing superfluid phase. Finally, in the region *HBF*, the ground state is in the α-like superfluid phase, the metastable state is in the normal phase.

Intersection of the continuous horizontal line *ADBF* corresponds to second-order phase transitions. Such phase transitions are already known from studies in the framework of the pair model[2,56] (which is a special case of our model for $g_4=0$). In the framework of the ESM, intersection of the boundary is replaced by a vertical line along g_2 (see Fig. 13) at the point ($g_2=0.2$, $g_4=0$).

Note also that along the line *ADBF* in our phase diagram two types of second-order phase transitions between the normal and pairing superfluid phases are possible: one for ground states in the region *HBDAOG*, and the other for metastable states in the region *HBF*. Intersection of the curve *CIBH* corresponds to first-order phase transitions of two types: from the pairing superfluid phase to the α-like superfluid phase (*CIB*), and from the normal phase to the α-like superfluid phase.

Some comments are appropriate here. The first is that our average-field approximation is not taken into account seriously for gaps slightly less than the cutoff (in our case $n+1$), in contrast to the situation with strong coupling. In particular, transition through the curve *CIBH*, which appears when $\sqrt{x}\geqslant 22$ [otherwise for Fig. 13 and $\sqrt{x}\geqslant 2(n+1)$], can indeed create certain difficulties. It is possible that a renormalization-group investigation will indicate whether or not an improved correlation energy reduces or strengthens this transition. In an alternative approach clarifying this point, one can consider the dependence of the controllable parameters g_2 and g_4, for which a natural cutoff is present. In any case, a large part of the phase diagram in Fig. 13 is in the domain of our approximation, so that at least part of the richness of behavior that we have found is guaranteed.

The new phase considered here, the α-like superfluid phase, lies in the part of the phase diagram in which g_4 is dominant (see Fig. 13), while the pairing superfluid phase is in the region with dominant g_2. Since g_4 is the coupling strength in the interaction H_4, which is in practice an interaction between one proton Cooper pair and one neutron Cooper pair, we have called this new phase an α-like superfluid phase.

4. PHASE TRANSITIONS AT FINITE TEMPERATURES

Since the concept of temperature was introduced[58] in nuclear physics, it has been intensively studied, both from the point of view of a formalism that includes temperature and from the point of view of understanding physical processes that can be described by means of this parameter. Although nuclear systems are finite, a large number of degrees of freedom can be excited at not too high energies. Therefore, a statistical treatment is needed. This fact was known from the initial stage of development of nuclear physics, basically for the description of reactions with neutrons and fission. This has now been supplemented with the field of heavy-ion physics, for which information is obtained in the same approximation. Levels above the yrast line[59,60] are mostly excited through collective states ($T=0$). Since the time needed to achieve thermal equilibrium is found to be less than the excitation time[59,60] of states above the yrast line, it is to be expected that in this excitation region the nucleus can be described by average-field models at finite temperature ($T\neq 0$). At the same time, it is found that the temperature is a suitable parameter for distinguishing phase transitions specific for the average field. Extensive variables are S (entropy), I (spin), and N_τ (number of nucleons of species τ), and intensive variables are T (temperature), w (quantum of rotational energy), and λ_τ (Fermi energy of interacting nucleons), which are Lagrangian parameters associated with S, I, and N_τ, respectively.

Thermodynamic potentials of various types can be introduced, for example, $G_I=E-TS-\omega I$, $G_\tau=E-TS-\lambda_\tau N_\tau$, and $G_{np}=E-TS-\Sigma_\tau\lambda_\tau N_\tau$ or $G_{Inp}=E-TS-\omega I-\Sigma_\tau\lambda_\tau N_\tau$. Analyzing the behavior of these thermodynamic potentials with respect to the intensive variables, we can determine (in the framework of the various approximations: HF,[61–63] HFB,[59,64] BCS + cranking model,[60,61,65] etc.) phase transitions, which may be of different types (and order), for example, a first-order phase transition from spherical to deformed shape,[62,63] a second-order phase transition from the normal to the superfluid (pairing) phase,[65,66] etc.

Gap equation at finite temperature

In our case, the thermodynamic (Gibbs) potential for the system of interacting nucleons has the form

$$\mathcal{G}=\hat{H}-\sum_\tau \lambda_\tau \hat{N}_\tau - k_B TS, \tag{63}$$

where $\hat{H}=H_0$ from (1) and

$$S=2\sum_\tau\sum_{s_\tau}\ln\{(1-\bar{n}_{s_\tau})^{\bar{n}_{s_\tau}-1}\bar{n}^{-\bar{n}_{s_\tau}}\}$$

$$=2\sum_\tau\sum_{s_\tau}\left\{\frac{1}{k_B T}\varepsilon_{s_\tau}\bar{n}_{s_\tau}-\ln(1-\bar{n}_{s_\tau})\right\} \tag{64}$$

is the entropy.[60] In these equations

$$\bar{n}_{s_\tau}=\left(1+\exp\frac{\varepsilon_{s_\tau}}{k_BT}\right)^{-1} \tag{65}$$

are the occupation numbers of the single-quasiparticle states, E_{s_τ} and ε_{s_τ} are the single-particle and single-quasiparticle energies, λ_{s_τ} are the Fermi energies for the interacting nucleons, k_B is Boltzmann's constant, and T is the temperature. We determine the single-quasiparticle Hamiltonian as follows:[60]

$$\tilde{H}=U_0+\sum_\tau\sum_{s_\tau\sigma_\tau}\varepsilon_{s_\tau}\alpha^\dagger_{s_\tau\sigma_\tau}\alpha_{s_\tau\sigma_\tau}, \tag{66}$$

where U_0 is a constant and the thermodynamic mean value of any operator $\hat{O}$ is defined by

$$\langle\hat{O}\rangle_0=\frac{\mathrm{Tr}\left(\hat{O}\exp\left(-\frac{\hat{H}}{k_BT}\right)\right)}{\mathrm{Tr}\exp\left(-\frac{\hat{H}}{k_BT}\right)}. \tag{67}$$

Using the thermodynamic mean values

$$\left\langle\sum_{s_\tau}\alpha^\dagger_{s_\tau\sigma_\tau}\alpha_{s_\tau\sigma_\tau}\right\rangle_0=2\bar{n}_{s_\tau}, \tag{68}$$

$$\langle A(s_\tau s'_\tau)\rangle_0=0, \tag{69}$$

$$P_\tau=\langle\hat{P}_\tau\rangle_0=\sum_{s_\tau}u_{s_\tau}v_{s_\tau}(1-2\bar{n}_{s_\tau}), \tag{70}$$

we write the Gibbs thermodynamic potential (63) in the form

$$\mathcal{G}=\sum_\tau\left\{2\sum_{s_\tau}(\tilde{E}_{s_\tau}-\lambda_\tau)[\bar{n}_{s_\tau}+v^2_{s_\tau}(1-2\bar{n}_{s_\tau})]-G_\tau P^2_\tau\right.$$
$$\left.-2k_BT\sum_{s_\tau}\left[\frac{1}{k_BT}\bar{n}_{s_\tau}\varepsilon_{s_\tau}-\ln(1-\bar{n}_{s_\tau})\right]\right\}-G_4P^2_pP^2_n. \tag{71}$$

In the limit $G_4\to0$, the expression (71) is identical to what is obtained in Refs. 60 and 65 in the framework of the pair model.

Applying the variational principle to this Gibbs potential,

$$\delta\mathcal{G}=\sum_{s_\tau}\left(\frac{\partial\mathcal{G}}{\partial v_{s_\tau}}\delta v_{s_\tau}+\frac{\partial\mathcal{G}}{\partial\bar{n}_{s_\tau}}\delta\bar{n}_{s_\tau}\right)=0, \tag{72}$$

subject to the condition $u^2_{s_\tau}+v^2_{s_\tau}=$, we obtain

$$\frac{\partial\mathcal{G}}{\partial v_{s_\tau}}=\frac{2(1-2\bar{n}_{s_\tau})}{u_{s_\tau}}\{(E_{s_\tau}-\lambda_\tau)2u_{s_\tau}v_{s_\tau}-(u^2_{s_\tau}-v^2_{s_\tau})\Delta_\tau\}=0, \tag{73}$$

where

$$\Delta_\tau=P_\tau(G_\tau+G_4P^2_{-\tau}) \tag{74}$$

and

$$\frac{\partial\mathcal{G}}{\partial\bar{n}_{s_\tau}}=2\{(E_{s_\tau}-\lambda_\tau)(u^2_{s_\tau}-v^2_{s_\tau})+2u_{s_\tau}v_{s_\tau}\Delta_\tau-E_{s_\tau}\}=0. \tag{75}$$

In the solution of the last two equations, we obtain for the single-quasiparticle energy the expression

$$\varepsilon_{s_\tau}=\sqrt{(E_{s_\tau}-\lambda_\tau)^2+\Delta^2_\tau} \tag{76}$$

and the occupation probability

$$\begin{pmatrix}u^2_{s_\tau}\\v^2_{s_\tau}\end{pmatrix}=\frac{1}{2}\left[1\pm\frac{E_{s_\tau}-\lambda_\tau}{\varepsilon_{s_\tau}}\right]. \tag{77}$$

The gap and constraint equations have the form[60,65]

$$\frac{1}{2}\{G_\tau+G_4P^2_{-\tau}\}\sum_{s_\tau}\frac{1-2\bar{n}_{s_\tau}}{\varepsilon_{s_\tau}}=1, \tag{78}$$

$$\sum_{s_\tau}\left\{1-(1-2\bar{n}_{s_\tau})\frac{E_{s_\tau}-\lambda_\tau}{\varepsilon_{s_\tau}}\right\}=N_\tau, \tag{79}$$

where N_τ is the number of particles of species τ that contribute to the superfluidity of the system. The solutions of the last two equations at the given temperature establish the phase to which the analyzed nucleus belongs.

New forms of phase transitions at finite temperatures

To understand the nature of the phase structure as a function of the temperature, we again use the homogeneous model (see Sec. 3).

The correlated Gibbs potential, like the correlation energy, has the form[67,68]

$$\varepsilon(g_2,g_4,t;x)\equiv\rho[\mathcal{G}(g_2,g_4,t;x)-\mathcal{G}(g_2,g_4,t;0)]$$
$$=4S_1(t;0)-4S_1(t;x)+4xS_{-1}(t,x)$$
$$-2g_2xS^2_{-1}(t,x)-g_4x^2S^4_{-1}(t,x)$$
$$-4t\sum_{k=-n}^{n+1}\{t^{-1}\varepsilon_k(x)\bar{n}_k(t,x)-\ln[1$$
$$-\bar{n}_k(t,\bar{x})]\}, \tag{80}$$

where

$$t=\rho k_BT, \tag{81}$$

$$S_j(x)=\frac{1}{2}\sum_{k=-n}^{n+1}[x+(k-1/2)^2]^{j/2}[1-\bar{n}_k(t,x)], \tag{82}$$

$$\bar{n}_k(t,x)=\left[1+\exp\frac{(x+(k-1/2)^2)^{1/2}}{t}\right]^{-1}, \tag{83}$$

$$\varepsilon_k(x)=[x+(k-1/2)^2]^{1/2}. \tag{84}$$

A similar expression for the gap (56) can be written in the form

$$F(g_2,g_4,t;x)=\frac{\partial\sigma(g_2,g_4,t;x)}{\partial x}=0. \tag{85}$$

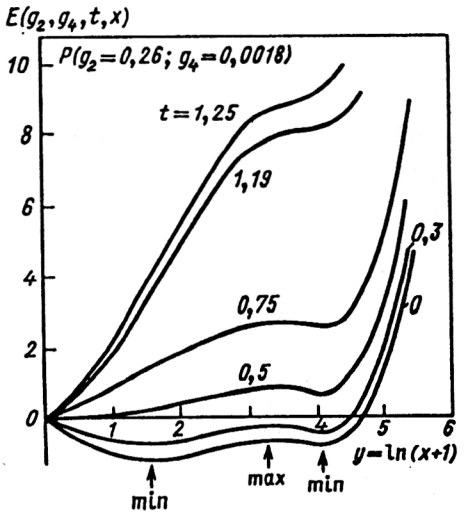

FIG. 14. Correlated Gibbs potential for the P nucleus (see the text) as a function of the gap parameter for various temperatures.

A phase diagram like the one in Fig. 13 is again very difficult to obtain, but one can analyze two hypothetical nuclei P ($g_2=0.26$, $g_4=0.00180$) and Q ($g_2=0.26$, $g_4=0.00183$), the first of which belongs to the pairing superfluid phase, and the second to the α-like superfluid phase (see Fig. 13). In Figs. 14–19 we see the phase transitions discussed in the previous section, analyzed for increasing temperatures. In the framework of the thermal approximation, the existence and characteristics of the normal and superfluid phases can be analyzed more clearly. A second-order phase transition between the pairing superfluid and normal phases exists when the temperature is increased to $t=0.51$ for the P nucleus.

A first-order phase transition between the α-like superfluid and normal phases exists when the temperature is increased to $t=0.58$ for the Q nucleus.

As can be seen from Figs. 16 and 17, there exist new critical temperatures corresponding to the α-like superfluid

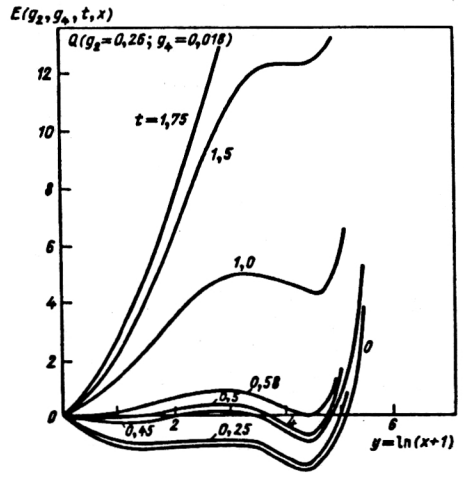

FIG. 15. Correlated Gibbs potential for the Q nucleus (see text) as a function of the gap parameter for different temperatures.

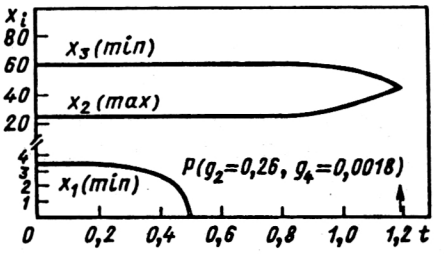

FIG. 16. Energy-gap parameters of the P nucleus (see the text) as a function of the temperature.

phase in addition to the well-known pairing critical temperatures (see Figs. 16–19 and Ref. 60).

Some other conclusions concerning phase transitions for metastable states (superfluid isomers) can be drawn on the basis of Figs. 14–19.

5. SOME APPLICATIONS OF THE ENLARGED SUPERFLUID MODEL

Nature of odd–even fluctuations of the charge radii of chains of isotopes of various nuclei

Some experimental data relating to odd–even fluctuations of the charge radii of chains of isotopes of various elements were given in Sec. 2. In this section, we shall attempt to give a model-dependent explanation of this effect.

For many years, nuclear charge radii have been the subject of intensive investigation.[7] From the liquid-drop model there follows an expression for the rms nuclear radii:

$$\langle r^2(A)\rangle^{1/2}=\sqrt{(3/5)}r_0(A)A^{1/3}, \tag{86}$$

where $r_0(A)$ has a weak A dependence:

$$r_0(A)=1.5+1.8A^{-2/3}-1.2A^{-4/3}. \tag{87}$$

However, modern techniques give rather large deviations from this law. Such measurements of the isotopic shifts have been made by means of optical spectroscopy,[7] laser spectroscopy,[11] or in μ-mesic atoms.[69]

Attempts at theoretical explanations have been based on allowance for the blocking effect of the ground state of nuclear vibrations by an odd neutron and allowance for blocking of pairing correlations together with polarization of the proton distribution by the neutrons. A first step in

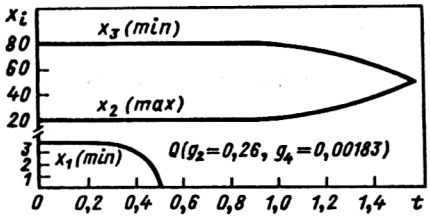

FIG. 17. Energy-gap parameters of the Q nucleus (see the text) as a function of the temperature.

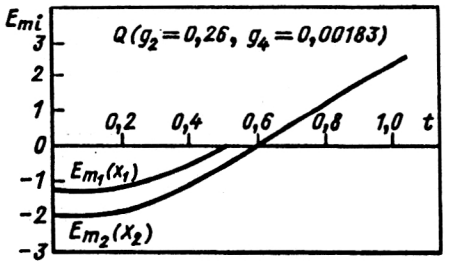

FIG. 18. Correlated Gibbs potential at points of minima for the P nucleus (see the text) as a function of the temperature.

the explanation of the deviations was taken in Ref. 70 in the framework of a model with pairing and quadrupole interactions and with phenomenological allowance for monopole and quadrupole polarizations of the core. In this case, the $B(E2)$ probabilities for even–even nuclei were reproduced. However, the staggerings were not. A staggering parameter[7] was introduced as a measurable magnitude of the deviations. Another explanation is that the staggering is a manifestation of the zero-point vibrations of the quadrupole vibrations, which are larger for odd nuclei.[71] However, the calculations, including phenomenological assumptions or fitting of parameters, give, in the best case, an effect that is too small.

Talmi's description

Talmi described the staggering by core polarization associated with a separable neutron–proton interaction that depends on three parameters (A,B,C). The charge radius is given by

$$\langle 0|r^2|0\rangle=\langle r^2\rangle_0+nC+\frac{1}{2}n(n-1)+\left[\frac{1}{2}n\right]B, \qquad (88)$$

where n is the number of neutrons in the j shell, and $[x]$ is the integer part of x. The parameters A, B, and C are fitted but have no physical meaning. For the case of the Pb isotopes, we see in Fig. 20 a comparison with experiment of the predictions of Talmi's model.

Zawischa's 2N model

Among other theoretical explanations, we mention application of the theory of finite Fermi systems with careful fitting of the single-particle energies to the problem of the

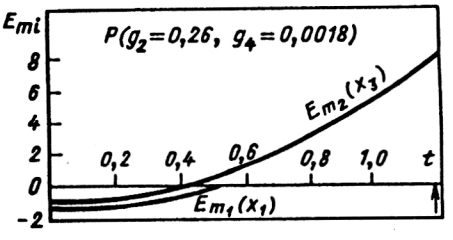

FIG. 19. Correlated Gibbs potential at points of minima for the Q nucleus (see the text) as a function of the temperature.

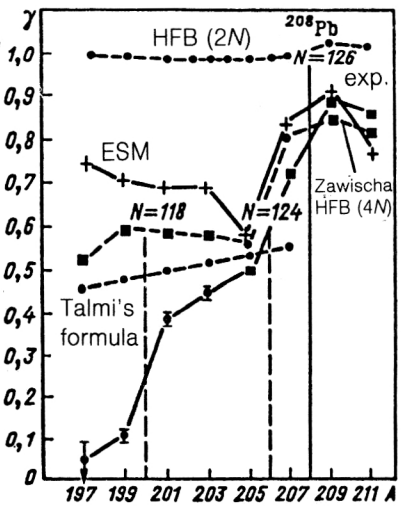

FIG. 20. The staggering parameters for lead isotopes as found experimentally[11] and calculated in the Talmi and Zawischa models and the ESM.

normal staggerings. To improve the agreement with experiment, it was postulated that the two-particle $(2N)$ interaction must be realistic.

Zawischa, Speth, and Pal,[49] using an effective density-dependent zero-range *ph* and *pp* interaction in the parametrization of Migdal and Lipkin,[89] successfully explained the structure and transition strengths for low-lying and high-lying states with $K^\pi=0^+$, 1^+, and 2^+ as well as for resonances with $K^\pi=0^-$ and 1^- for deformed rare-earth nuclei in the MHF framework. This model, applied to the problem of staggering the charge radii,[74] gives practically no staggering (see Table II and Fig. 20).

Zawischa's 2N+4N model

A more interesting suggestion was that of the existence of a four-nucleon interaction (two protons and two neutrons) in addition to the two-nucleon interaction. This led to the first positive results in the staggering problem, which were obtained by Zawischa *et al.*[12,73–75]

To the Hamiltonian of the theory of finite Fermi systems, those authors added the four-nucleon interaction term

$$\Xi=\xi\delta(\mathbf{r}_1-\mathbf{r}_2)\delta(\mathbf{r}_1-\mathbf{r}_3)\delta(\mathbf{r}_1-\mathbf{r}_4)$$
$$\times\tfrac{1}{2}[1-p_\sigma(1,2)]\tfrac{1}{2}[1-p_\sigma(3,4)], \qquad (89)$$

where ξ, the coupling constant, was chosen to reproduce the staggering. The term (89) presupposes a mechanism that couples strongly the pairing properties of the protons and neutrons, like the term H_4 (13) in the Hamiltonian (9) of our model.

In the framework of this approach, the staggering mechanism (see Table IV and Figs. 20 and 21) is explained by corrections to the normal density of the protons due to the parts of the self-consistent field that are generated by

TABLE IV. Comparison of experimental[7-11] isotopic shifts $\delta\langle r^2\rangle$ (fm^2) with results of calculations in the HFB($2N$) and HFB($4N$) models and the ESM. For the explanation, see the text.

A	HFB ($2N$)	Zawischa[49]	ESM	Experiment	
				Ref. 6.	Ref. 10
197	0,052	0,034	0,055	−0,037	0,002
198	0,052	0,098	0,088	0,082	0,082
199	0,052	0,033	0,050	0,009	0,005
200	0,043	0,075	0,091	0,085	0,088
201	0,053	0,032	0,048	0,023	−0,0007
202	0,053	0,074	0,088	0,080	0,081
203	0,054	0,031	0,043	0,027	0,014
204	0,053	0,074	0,078	0,080	0,081
205	0,055	0,029	0,034	0,029	0,026
206	0,055	0,077	0,082	0,077	0,079
207	0,057	0,054	0,058	0,045	0,044
208	0,063	0,075	0,078	0,047	0,074
209	0,066	0,081	0,078	0,091	0,093
210	0,057	0,116	0,090	0,112	0,117
211	0,065	0,077	0,068	—	0,089
212	0,056	0,115	0,117	—	0,115
213	0,064	0,073	0,065	—	—
214	0,057	0,115	0,112	—	—

the four-particle interaction. These corrections are functions of the neutron pair density.[12,73-75]

Description in the enlarged superfluid model

In the framework of the ESM,[15-18] the staggering is generated by corrections to the proton density due to the mutual behavior of the proton and neutron superfluidities through a four-nucleon interaction [see Eq. (29)] and blocking of the pairing and α-like correlations. The charge radius staggering in the isotopes of lead (which is a magic nucleus) is one of the most important cases for the ESM because Belyaev's critical condition (see Sec. 3) will not be satisfied when the interaction H_4 is switched off, and the proton system will be in the normal phase. When the interaction H_4 is absent, proton superfluidity is induced by the already established neutron superfluidity. Therefore, the charge-radius staggering is associated with induced proton superfluidity and does not introduce changes[74] in the canonical basis.[57]

Table IV and Fig. 20 show the isotopic shifts of the

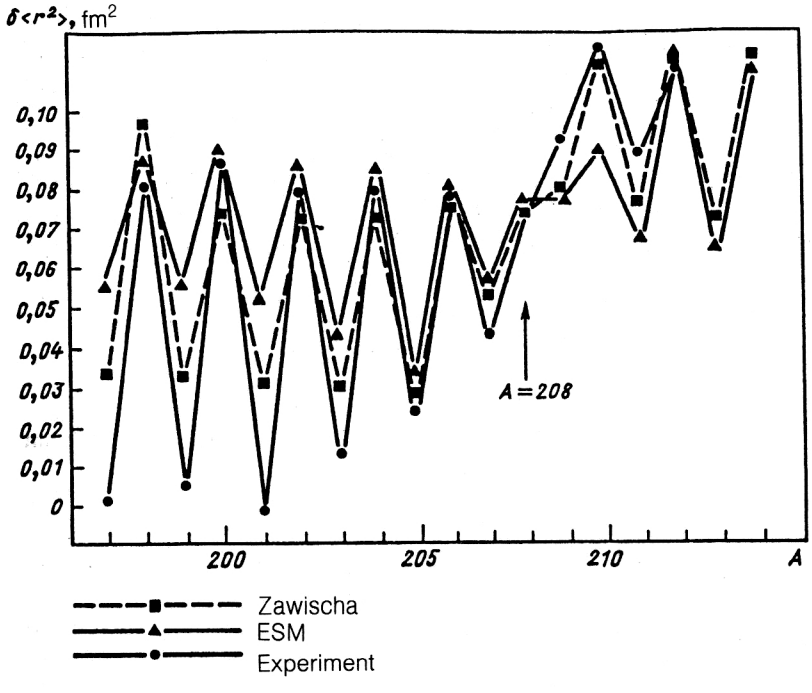

FIG. 21. Odd–even staggering of mean square charge radii for lead isotopes. The experimental data are taken from Ref. 11.

TABLE V. Experimental and calculated (see the text) energies of the first low-lying 0^+ states, divided into two superfluid bands.

Superfluid band	$I^{\pi}K$	E_{exp}, MeV	E_{theor}, MeV
Ground state	0^+0	0	0
	0^+0	0,685	0,670
Isomer state	0^+0	1,082	0,837
	0^+0	1,737?	4,500

charge radii for nuclei of lead isotopes. The results of calculations based on the HFB method with a density-dependent two-nucleon interaction, on the basis of the HFB method with inclusion of Zawischa's four interactions[73] and on the basis of our ESM, are compared with experimental data.[7,11] In the calculations, we use the single-particle energies and wave functions of the Woods–Saxon potential for very small deformations ($\beta_{20}=0.005$ and $\beta_{40}=0$); the parameters of the potential are taken from Ref. 3 (p. 21 of the Russian original), and the ESM parameters are $C_p=12$ MeV, $C_n=30$ MeV, $C_4=12$ MeV.

Despite the quantitative differences between Zawischa's model and the ESM, the tendencies are qualitatively the same (see Table IV and Figs. 20 and 21). This shows that at least in the region of lead the ESM describes a large part of the staggering amplitude.

Superfluid isomers

We have chosen the term *superfluid isomers* by analogy with fission shape isomers, which are in fact shape isomers corresponding to a second minimum of the potential energy with respect to elongation.[76] An analogy can be made in the spirit of Bohr–Mottelson symmetry breaking.[2] The appearance of pair rotations,[77] for example, as elementary-excitation modes, is associated with breaking of the symmetry of the nucleon-number conservation. This type of symmetry breaking generates a superfluid phase of nuclei with nonzero static deformation Δ of the pairing fields.

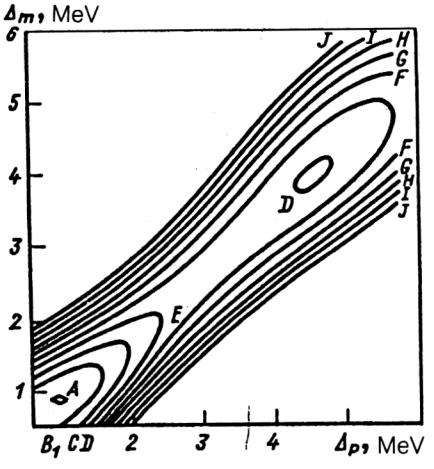

FIG. 22. Correlation energy with respect to the proton and neutron energy gap. The two minima have the coordinates described in the text: $A=-918.35$ MeV, $B=-918.07$ MeV, $C=-917.80$ MeV, $D=-917.52$ MeV, $E=-917.24$ MeV, $F=-916.96$ MeV, $G=-916.69$ MeV, $H=-916.41$ MeV, $I=-916.13$ MeV, $J=-915.85$ MeV.

There is here a complete analogy with the presence of a rotation spectrum in deformed nuclei, i.e., the breaking of the rotation symmetry leads to the appearance of a nonzero static deformation β of the self-consistent average field and, therefore, to rotational levels in the nuclear excitation spectrum. The value of the deformation parameter β corresponds to an overall minimum of the system's potential energy with respect to elongation, and this minimum determines the ground state. Fission isomers and other shape isomers correspond to a local minimum of the potential energy. By analogy, we can obtain a second (local) minimum as a function of the static deformations $\Delta_{p(n)}$ of the pairing field, as we shall show in what follows.

Solution of gap equations in a realistic case

Our task is to minimize the energy functional, for example, for an even–even nucleus [see (26)],

$$W(u_{s_p},v_{s_p},u_{s_n},v_{s_n})=\sum_{i=p,n}\left(2\sum_{s_i}E_{s_i}v_{s_i}^2-G_i\chi_i^2\right)-G_4\chi_p^2\chi_n^2, \tag{90}$$

$$\chi_i=\sum_{s_i}u_{s_i}v_{s_i}, \tag{91}$$

$$u_{s_i}^2+v_{s_i}^2=1 \tag{92}$$

with respect to the variational parameters v_{s_i}, which satisfy the condition

$$\sum_{s_i}2v_{s_i}^2=N_i, \tag{93}$$

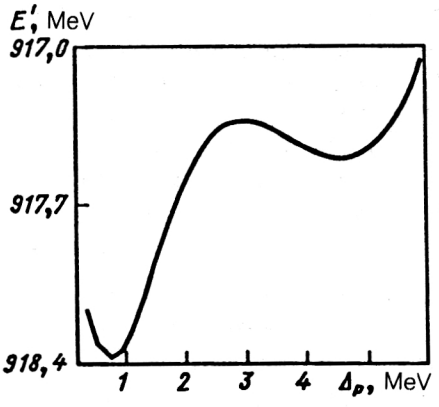

FIG. 23. Profile of correlation energy as a function of the proton energy gap along the path between the two minima.

where N_i $(i=p, n)$ is the number of nucleons contained in the truncated energy interval, and E_{s_i} are the renormalized single-particle energies. This problem is analogous to minimization of the functional

$$F(v_{s_p}, v_{s_n}, \lambda_p, \lambda_n) = W(v_{s_p}, v_{s_n}) - \sum_{i=p,n} \lambda_i \left(2 \sum_{s_i} v_{s_i}^2 - N_i \right) \tag{94}$$

with respect to $v_{s_{p(n)}}$ and $\lambda_{p(n)}$, and therefore, taking $\lambda_i = \lambda_i(\Delta_i^2)$ and the gap equations (29), or minimizing the functional

$$W' = W[v_{s_p}(\Delta_p^2), v_{s_n}(\Delta_n^2), \lambda_p(\Delta_p^2), \lambda_n(\Delta_n^2)] \tag{95}$$

with respect to $\Delta_{p(n)}^2$, we take into account the condition (93), where the functions $v_{s_{p(n)}}$ must have the parametrization (30).

In our case, the role of the potential energy for the fission isomers will be played by W' as a function of $\Delta_{p(n)}$, the static deformations of the pairing and four-nucleon fields.

We now analyze the case of $^{152}_{62}Sm_{90}$. This nucleus has well-defined rotational bands[78] corresponding to the following intrinsic K_π states: ground state 0^+; β-vibrational state 0^+ ($E=0.685$ MeV); γ-vibrational state 2^+ and octupole vibrational state 1^-. There exist three additional intrinsic 0^+ states with $E_2=1.082$ MeV, $E_3=1.656$ MeV, $E_4=1.736$ MeV. On the second 0^+ excited state ($E_2=1.082$ MeV) there is based a rotational band with moment of inertia less than the moments of inertia of the ground and β-rotational bands. This second 0^+ excited state ($E_2=1.082$ MeV) may be a first indication of the existence of a superfluid isomer in this nucleus, since the second minimum corresponds to a large gap parameter (see Table V and Figs. 22 and 23) and therefore, it is understood, a smaller moment of inertia.

The possible interpretation of this excited state as a two-phonon β state, two-quasiparticle state, or neutron pairing vibrational state contradicts the experimental data on the position of the energy level, the moment of inertia, and the electromagnetic transition strengths (Fig. 24 and Ref. 78).

Calculations of the theoretical parameters, given in Table V and in Fig. 22, were made[16] on the basis of the single-particle Woods–Saxon scheme with deformation ($\beta_2=0.3$ and $\beta_4=0.05$) and shape parameters taken from Ref. 3, and with ESM parameters $C_p=22.4$ MeV, $C_n=16.2$ MeV, $C_4=28$ MeV. For the global minimum of W' (Fig. 22), corresponding to the ^{152}Sm ground state, the gaps and Fermi energies were found to be $\Delta_{p_1}=0.597$ MeV, $\lambda_{p_1}=6.938$ MeV, $\Delta_{n_1}=0.586$ MeV, and $\lambda_{n_1}=6.372$ MeV, whereas for the second (local) minimum, of the superfluid isomer state, they are $\Delta_{p_2}=4.567$ MeV, $\lambda_{p_2}=7.117$ MeV, $\Delta_{n_2}=3.920$ MeV, and $\lambda_{n_2}=-6.508$ MeV.

It is found that the ratio of the $E0$ probabilities of the isomer-state–ground-state and vibrational-state–ground-state transitions will be rather large ($\cong 250$),[79] in agreement with the interpretation of the second 0^+ excited state in ^{152}Sm as a superfluid isomer.

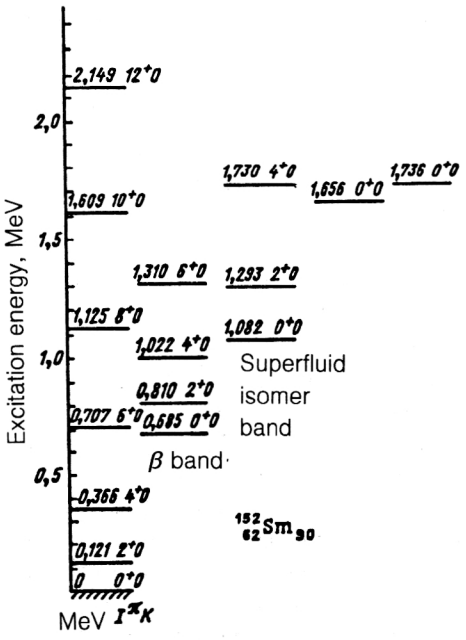

FIG. 24. Experimental rotational bands based on the ground and first two 0^+ excited states of ^{152}Sm.

Discussion of the moment of inertia

The experimental value of the moment of inertia of the second 0^+ excited state is half the value for the ground-state rotational band ($I_{\text{g.s.}}=24.8$ MeV^{-1} and $I_{\text{isomer}}=14.2$ MeV^{-1}). This indication is confirmed by the fact that the moment of inertia predicted by the superfluid model decreases with increasing gap parameter ($\Delta_{p(n)}$). Alternatively, in our case the gap parameter for the global minimum (ground state) does not differ too strongly from that predicted by the quasiparticle–phonon nuclear model (QPNM).[3] If the moment of inertia[53] is calculated in accordance with Belyaev's formula, we obtain a value too small compared with the experiment, though our calculations did not take into account the possible change of the deformation of the average field in going from the ground state to the isomer state. There are indications (Refs. 50, 51, 80, and 81) that the isomer state has a much smaller deformation (and even $\beta=0$) than the ground state. This may increase the calculated moment of inertia in the ESM for the parameters that we use for the superfluid isomer.

Isomer superfluid band

Applying now the MHF treatment[3] for the Hamiltonian (9) of Ref. 15, in which the part H' (14) is restricted to the quadrupole–quadrupole interaction, we calculate the energies of β-vibrational states (see Table V) based on the ground and superfluid isomer states. The existence of a first MHF root for the superfluid isomer at lower energies than the first band confirms the correctness of our model in the description of the superfluid isomer.

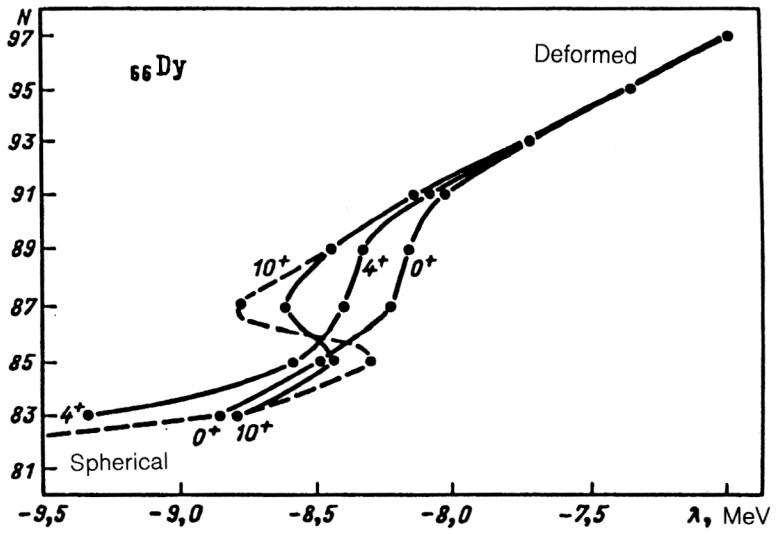

FIG. 25. The "measured" backbending curve: the number of neutrons relative to the neutron Fermi energy, taken as half the two-neutron separation energy for Dy isotopes.

The solutions to the gap equations discussed above, corresponding to global and local minima, determine the pairing and α-like superfluid phases, respectively. The ground state of the pairing superfluid band contains rotational bands based on the ground, β-vibrational (0.685 MeV), γ-vibrational, and octupole vibrational states, whereas the superfluid isomer band contains at least a rotational band based on the second 0^+ excited state ($E_2=1.082$ MeV) (see Figs. 22–24 and Table V).

New types of nuclear phase transitions

It is firmly believed that the shape of nuclei in the ground state in the region of Sm changes from almost spherical to almost spheroidal (deformed) as the neutron number is changed from 82 to 94. The reasons for such a transition are extremely varied and include changes in the structure of the low-lying levels,[78] in the probabilities of transitions between the first excited and ground states,[82] and the systematics of the binding energies.[83] These data indicate an abrupt transition between $N=88$ and $N=90$. Figure 25 shows the "measured" backbending curve in this region (namely, the number of neutrons with respect to the neutron Fermi energy, taken as half the two-neutron separation energy), which can be interpreted as a phase transition. The steepness of the transition reflects the fact that ^{152}Sm ($N=90$) is "very deformed" with a clearly distinguished ground-state rotational band (the ground-state moment of inertia is $I\cong 25$ MeV^{-1}, which confirms the value $\beta\cong 0.3$ of the deformation parameter), while ^{150}Sm ($N=88$) is a spherical nucleus in the ground state.[79]

The (t, p) and (p, t) transfer reactions in the region of samarium

Hinds *et al.*[84] found that in (t, p) stripping reactions on the spherical nucleus ^{150}Sm certain "spherical states" of ^{152}Sm will be strongly excited. They observed a large cross section (75% compared with the reaction to the ground state) for the (t, p) stripping reaction, leading to a state

TABLE VI. Comparison of cross sections for (p, t) and (t, p) transfer reactions leading to the 0^+ final state in Sm isotopes. The cross section of the ^{152}Sm$(p, t)^{150}$Sm reaction to the ground state is normalized to the cross section of the inverse ^{150}Sm$(t, p)^{152}$Sm reaction.

A_k	K_f, MeV	$\sigma(p, t)$, arb. units	$\sigma(t, p)$, arb. units
146	0	349	290
	2,611	< 4	90
148	0	428	—
	1,426	75	—
	1,923	4	—
	2,206	14	—
	2,358	27	—
150	0	190	570
	0,738	156	140
	1,255	111	0
152	0	282	190
	0,688	79	140
	1,091	< 3	130
	1,662	4	0
154	0	—	300
	1,117	—	30
	1,218	—	100
156	0	—	300
	1,068	—	20

0^+, $E_x=1.082$ MeV, a result which usually leads to the conclusion that the considered nuclear state has a spherical shape. Somewhat later, Maxwell *et al.*,[85] using the inverse ^{152}Sm (p, t) ^{150}Sm reaction, observed an analogous situation on occupation of the 0^+ ($E_x=1.28$ MeV) state in ^{150}Sm and concluded that this ^{150}Sm state is deformed. Such a conclusion can be drawn from analysis of the rotational bands[78] corresponding to the ground state and the first two excited 0^+ states in ^{150,152}Sm. These investigations were repeated in Refs. 80 and 86, and more convincing experimental data (see Table VI) were found.

Interpretation of phase transitions as shape transitions

For a long time, it was difficult to explain the experimental data in going from $N=88$ to $N=90$ by all nuclear models. Attempts to explain the data were made by Mottelson and Nilsson,[87] on the basis of a change in the properties of the self-consistent field due to the presence of a $1h_{11/2}$ intruder state in the proton system. Almost all the models proposed later follow the idea of treating the pairing properties as practically unchanged. In Refs. 50 and 51, the change was regarded as a phase transition from a spherical to a deformed shape in going from ^{150}Sm to ^{152}Sm (for the ground states) and in the other direction if we go from the ground states to the second 0^+ states. Kumar[50] developed a time-dependent HFB pairing + quadrupole model, using it first for the energy levels and the electromagnetic moments W, O_s, and P_t, and then modifying and extending it for states with higher angular momenta. He made a comparison with experiment for the energy levels, $B(E2)$ probabilities, quadrupole moments, magnetic moments, electric monopole transition moments, isomer shifts, and the ratios $E2/M1$ and $E0/E2$ for the nuclei ^{150}Sm and ^{152}Sm. Spectroscopic factors for single-proton, single-neutron, and two-proton transfer reactions were given. He gave a microscopic and collective explanation of the phase transition from the vibrational-type spectrum in ^{150}Sm to the rotational-type spectrum in ^{152}Sm. He attempted to introduce shape coexistence, but found that in such a model the $E2$ branching ratios are not satisfied.

Kishimoto and Tamura developed a boson technique of Belyaev–Zelevinskiĭ expansions up to the sixth order. They applied such an expansion up to the fourth order[51] to nuclei in the region of samarium. Despite the almost ideal agreement with the experimental data obtained in that study, it may be suspected that this good agreement was obtained only because of the different sets of parameters that were used for different nuclei, and/or the convergence of the Belyaev–Zelevinskiĭ expansion may be suspect.

The (p, t) and (t, p) reactions considered above can, however, be reproduced only under the assumption[88] that the wave functions of the ground and first two excited states of ^{150,152}Sm are superpositions of two wave functions of Nilsson+BCS type that depend on different deformations (β) of the self-consistent field and leave the pairing properties unchanged. The contribution of each component to the superposition is found by fitting the transfer

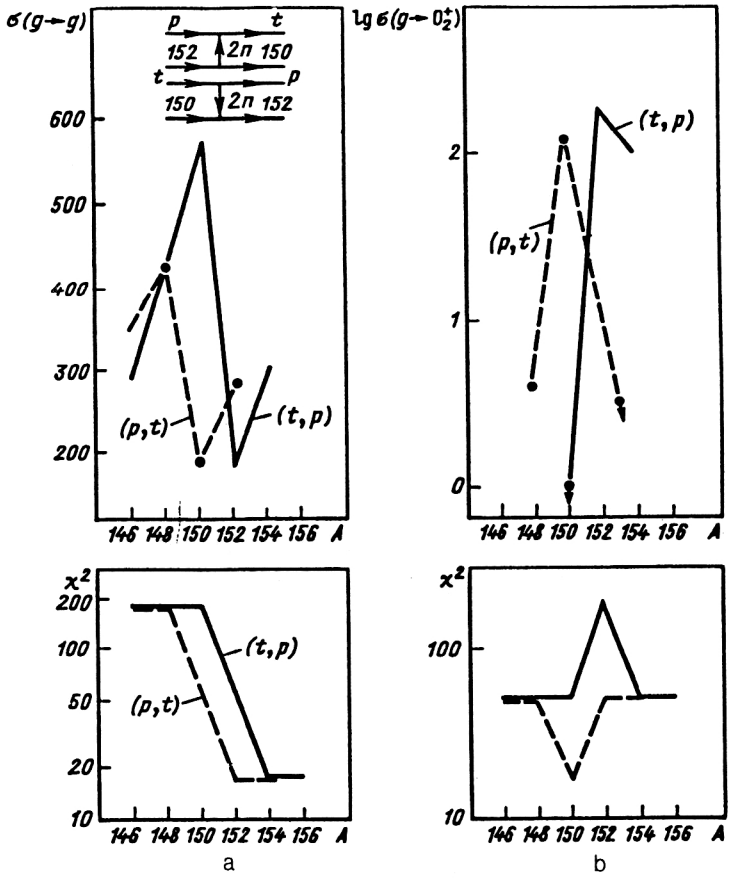

FIG. 26. Experimental cross sections (σ) and spectroscopic factors (χ^2) for (p,t) and (t,p) transitions: a) ground-state–ground-state; b) ground-state–second-0^+-state.

reaction data. A hybrid model of this kind contradicts the microscopic treatment of Refs. 50 and 51.

Interpretation of experimental data on the basis of a phase shift between two superfluid phases

Although the theories we have considered above are very complicated, none of them can be used to analyze the specific properties of the neutron–proton interaction in nuclei and beautiful specific experimental data such as the staggering of the charge radii of the isotopes of a given element. Kumar[50] found, for example, a discrepancy for ^{152}Sm between theory and experiment by a factor of three. This gives hope that our term H_4 in Eq. (13) could play an important role in describing the phase transition from ^{150}Sm to ^{152}Sm.

Figure 26 gives a possible explanation of this phase transition as a transition between an α-like superfluid phase and a pairing superconducting phase. It was assumed in the calculations that the ^{150}Sm ground state belongs to the former (with large gap parameters; see Fig. 22), and the ^{152}Sm ground state to the latter (small gap parameters; Fig. 22).

Figures 22a and 26b show the experimental data[86] and reproduce the spectroscopic factors for the *pt* and *tp* processes.

In the calculations, we used the same model parameters as earlier for fixed β.

The realistic calculations include variations both in the self-consistent field (for example, β) and in the properties of the pairing field ($\delta_{p(n)}$).

CONCLUSIONS

We have considered the influence of pairing and dynamical α-like correlations on the structure of nuclear states in the framework of the enlarged superfluid model. We have compared the ESM with other contemporary models of nuclear structure such as the quasiparticle–phonon model, the interacting boson model, the time-dependent HFB method, the HFB method, and Migdal's model of finite Fermi systems. We have obtained new gap equations. The phase structure is enriched by a new superfluid phase, the so-called α-like superfluid phase, which is dominant in α correlations. New first- and second-order phase transitions have been predicted. A first-order phase transition between the α-like superfluid phase and the pairing superfluid phase is observed in the region of Sm. New isomer types are predicted, so-called superfluid isomers with their own bands of elementary excitations. One of them is observed in ^{152}Sm. These isomers correspond to a second (local) minimum of the correlation energy with respect to pairing deformations and are analogous to fission or superdeformed (shape) isomers corresponding to a second (local) minimum of the potential energy with respect to the elongation in the nuclear shape. In the region of heavy nuclei, the superfluidities of the neutron and proton systems can generate each other. This leads to an explanation of the odd–even staggerings of the charge radii in chains of isotopes of various nuclei. The fact that the reduced α-decay width (γ^2) of neutron-deficient Pb isotopes is almost equal to the γ^2 value for α decays of the actinide region induces, as discussed above, the neutron superfluidity in the proton system. The ESM can explain such exotic data, especially in the region of magic nuclei. In the framework of the ESM, one can find a natural microscopic explanation of the scissors mode, which is dominant in the $K^\pi = 1^+$ structure of magnetic states.[90,91]

I thank Professor V. G. Solov'ev (JINR, Dubna) for constant support and helpful criticism over many years of collaboration. I also thank Professor Bisetti for some valuable discussions and hospitality at the Institute in Florence, where a large part of this paper was written. I also thank Professor Bosio, Professor Stanescu, Professor Ciofi del Atti, and Professor Salte for hospitality at the Sanita-Ris INFN, where some of the calculations presented in this paper were made. I am grateful to my colleagues Dr. Bulboaca, Dr. Carstoiu, and Dr. Horoi at the Theoretical Department of the Bucharest Institute of Atomic Physics and Dr. S. Ivanova at the JINR for many stimulating discussions and helpful collaboration. I am grateful to Professor Fond of Trieste for constant support and criticism. I thank Professor Salam, the IAEA, and UNESCO, for hospitality at the International Center for Theoretical Physics (Trieste), where this work was completed.

[1] A. Bohr, B. Mottelson, and D. Pines, Phys. Rev. **110**, 936 (1958).
[2] A. Bohr and B. Mottelson, *Nuclear Structure*, Vol. II (Benjamin, New York, 1975).
[3] V. G. Solov'ev, *Theory of Complex Nuclei* (Pergamon Press, Oxford, 1976) [Russ. original, Nauka, Moscow, 1971].
[4] F. A. Gareev, S. P. Ivanova, V. G. Solov'ev *et al.*, Fiz. Elem. Chastits At. Yadra **4**, 357 (1973) [Sov. J. Part. Nucl. **4**, 148 (1973)].
[5] A. L. Goodman, Adv. Nucl. Phys. **13**, 263 (1970).
[6] J. Bardeen, L. N. Cooper, and J. R. Schreiffer, Phys. Rev. **108**, 1175 (1957).
[7] K. Heilig and A. Steudel, At. Data Nucl. Data Tables **14**, 613 (1974).
[8] I. Angeli and M. Csaltos, Nucl. Phys. **A288**, 480 (1977).
[9] A. Andl, K. Bekk, S. Göring *et al.*, Phys. Rev. C **26**, 2194 (1982).
[10] R. C. Thompson, M. Anselment, K. Bekk *et al.*, J. Phys. G **9**, 443 (1983).
[11] M. Anselment, W. Faubel, S. Göring *et al.*, Nucl. Phys. **A451**, 471 (1986).
[12] D. Zawischa, Phys. Lett. **155B**, 307 (1985).
[13] A. Arima and F. Iachello, Adv. Nucl. Phys. **13**, 139 (1984).
[14] D. Janssen, R. V. Jolos, and F. Donau, Nucl. Phys. **A224**, 93 (1974).
[15] O. Dumitrescu, Nuovo Cimento **A104**, No. 7 (1991); Preprint IC/90/248, ICTP, Trieste (1990).
[16] O. Dumitrescu and M. Horoi, Nuovo Cimento **A103**, 653 (1990).
[17] O. Dumitrescu, in *Neutron Induces Reactions. Proc. of the 1985 Smolenice Symposium, Smolenice–Bratislava*, edited by J. Kristiak and E. Betak (Reidel and Veda, 1986), p. 119; *Gjoletchitze–Bulgaria–Nuclear Theory Workshop*; Bulg. J. Phys. **14**, 418 (1987).
[18] M. Apostol, I. Bulboaca, F. Carstoiu *et al.*, Nucl. Phys. **A470**, 64 (1987); Europhys. Lett. **4**(2), 197 (1987).
[19] O. Dumitrescu, Fiz. Elem. Chastits At. Yadra **10**, 377 (1979) [Sov. J. Part. Nucl. **10**, 147 (1979)].
[20] A. Bulgac and O. Dumitrescu, in *Proc. of the Roumanian Meeting of Physics* (ICEFIZ, Bucharest, 1979), p. 30.
[21] A. Bulgac, S. Holen, F. Carstoiu, and O. Dumitrescu, Nuovo Cimento **A70**, 142 (1982).
[22] A. Bulgac, F. Carstoiu, O. Dumitrescu, and S. Holan, in *Nuclear Physics Proc. 1081—Trieste Workshop*, edited by C. H. Dasso, R. A. Broglia, and A. Winter (North-Holland, Amsterdam, 1981), p. 295.

[23] A. Bulgac, F. Carstoiu, O. Dumitrescu, and S. Holan, in *Proc. of the Berkeley Conf. on Nuclear Physics*, edited by I. Diamond and J. O. Rasmussen, Sec. A, Vol. 1 (Nuclear Physics, 1980), p. 354.
[24] F. Carstoiu, O. Dumitrescu, G. Stratan, and M. Braic, Nucl. Phys. **A441**, 221 (1985).
[25] J. O. Rasmussen, in *α, β, and γ-Ray Spectroscopy*, edited by K. Seigbahn (North-Holland, Amsterdam, 1968), p. 701.
[26] P. B. Price, Ann. Rev. Nucl. Part. Sci. **39**, 19 (1989).
[27] F. Barranco, G. F. Bertch, R. A. Broglia, and E. Vigezzi, Nucl. Phys. **A512**, 253 (1980).
[28] D. M. Brink, in *Intern. School of Physics, Enrico Fermi*, Vol. 37 (1966), p. 247.
[29] J. A. Wheeler, Phys. Rev. **32**, 1083 (1937).
[30] K. Wildermuth and Th. Kanellopoulos, Nucl. Phys. **7**, 150 (1958).
[31] G. C. Phillips and T. A. Tombrello, Nucl. Phys. **19**, 555 (1960).
[32] V. I. Kukulin, V. G. Neudatchin, and Yu. F. Smirnov, in *Clustering Phenomena in Nuclei*, Vol. 3 (Vieweg Verlag, Braunschweig, 1982).
[33] K. Wildermuth and Y. C. Tang, in *A Unified Theory of the Nucleus* (Vieweg Verlag, Braunschweig, 1977).
[34] Y. Fujiwara and Y. C. Tang, Phys. Rev. C **31**, 342 (1985).
[35] M. V. Michailovic, in *Proc. of the Fourth Intern. Conf. on Clustering Aspects of Nuclear Structure and Nuclear Reactions* (Chester, 1984), p. 35.
[36] R. R. Betts, Phys. Rev. C **16**, 1617 (1977).
[37] Y. K. Gambhir, P. Ring, and P. Schuck, Phys. Rev. Lett. **51**, 1235 (1983).
[38] A. M. Lane and R. G. Thomas, Rev. Mod. Phys. **30**, 257 (1958).
[39] A. Arima, in *Proc. of the Fourth Intern. Conf. on Clustering Aspects of Nuclear Structure and Nuclear Reactions*, Vol. 47 (Winnipeg, 1978), p.1.
[40] A. B. Migdal, *Theory of Finite Fermi Systems and Applications to Atomic Nuclei*, transl. of 1st Russ. ed. (Interscience, New York, 1967) [Russ. original, Nauka, Moscow, 1965].
[41] I. Talmi, Rev. Mod. Phys. **34**, 704 (1962); in *Progress in Particle and Nuclear Physics*, Vol. 9, edited by D. Wilkinson (Pergamon Press, Oxford, 1983), p. 27; *Interacting Bosons in Nuclei* (Plenum Press, New York, 1979), p. 79.
[42] R. F. Casten, *Nuclear Structure from a Simple Perspective* (New York, 1990).
[43] M. Girog and P. G. Reinhard, Phys. Lett. **117B**, 1 (1982).
[44] J. Dobaczewski, H. Flocard, and J. Treiner, Nucl. Phys. **A422**, 103 (1984).
[45] W. H. King and M. Wilson, J. Phys. G **11**, 143 (1985).
[46] K. Toth, Y. A. Ellis-Akovali, C. R. Bingham *et al.*, Phys. Rev. Lett. **53**, 1623 (1984).
[47] K. Heide *et al.*, Nucl. Phys. **A466**, 189 (1987).
[48] V. G. Soloviev, Report E4-90-119, JINR, Dubna (1990).
[49] D. Zawischa, J. Speth, and D. Pal, Nucl. Phys. **A311**, 445 (1978).
[50] K. Kumar, Nucl. Phys. **A231**, 189 (1974).
[51] T. Kishimoto and T. Tamura, Nucl. Phys. **A192**, 246 (1972); **A270**, 317 (1976).
[52] D. R. Bes and R. A. Broglia, Phys. Rev. C **3**, 2349 (1971).
[53] S. T. Belyaev, K. Dan. Vidensk. Selsk. Mat.-Fys. Medd. **31**, No. 11 (1959).
[54] A. H. Wapstra and G. Audi, Nucl. Phys. **A432**, 1 (1985).
[55] F. A. Gareev, S. P. Ivanova, L. A. Malov, and V. G. Soloviev, Nucl. Phys. **A171**, 131 (1971).
[56] D. R. Bes and R. A. Broglia, in *Proc. of the Intern. School of Physics Enrico Fermi*, Varenna, 1976, edited by A. Bohr and R. A. Broglia (North-Holland, Amsterdam, 1977), p. 55.
[57] P. Ring and P. Schunk, *The Nuclear Many Body Problem* (Springer-Verlag, Berlin, 1980).
[58] B. F. Bayman, Nucl. Phys. **15**, 33 (1960).
[59] A. I. Goodman, Nucl. Phys. **A352**, 30, 45 (1981).
[60] A. V. Ignatyuk, *Statistical Properties of Excited Nuclei* [in Russian] (Énergoatomizdat, Moscow, 1983).
[61] K. Tanabe, K. Sugawara-Tanabe, and H. J. Mang, Nucl. Phys. **A357**, 20, 45 (1981).
[62] M. Brak and P. Quentin, Nucl. Phys. **A361**, 35 (1981).
[63] U. Mosel, P. G. Zint, and K. H. Passler, Nucl. Phys. **A236**, 252 (1974).
[64] A. L. Goodman, Nucl. Phys. **A369**, 365 (1981).
[65] O. Civitarese, G. C. Duessel, and R. P. J. Perazzo, Nucl. Phys. **A404**, 15 (1983).
[66] I. L. Egido, P. Ring, S. Iwasaki, and H. J. Mang, Phys. Lett. **154B**, 18 (1985).
[67] I. Brandus, I. Bulbuaca, O. Dumitrescu, and M. Horoi, Communication E4-87-48, JINR, Dubna (1987).
[68] F. Carstoiu, O. Dumitrescu, I. Brandus *et al.*, Preprint IC/88/17, ICTP, Trieste (1988).
[69] E. B. Shera, M. V. Hoehn, G. Fricke, and G. Mallof, Phys. Rev. C **39**, 195 (1989).
[70] R. A. Uher and R. A. Sorensen, Nucl. Phys. **86**, 1 (1966).
[71] B. S. Reehal and R. A. Sorensen, Nucl. Phys. **A161**, 385 (1971).
[72] I. Talmi, Nucl. Phys. **A423**, 189 (1984).
[73] D. Zawischa, U. Regge, and R. Stapel, Phys. Lett. **185B**, 299 (1987).
[74] D. Zawischa and J. Specht, Phys. Rev. Lett. **36**, 843 (1976).
[75] U. Regge and D. Zawischa, Phys. Rev. Lett. **61**, 149 (1988).
[76] S. Polikanov, V. A. Druin, V. A. Karnaukhov, *et al.*, Zh. Eksp. Teor. Fiz. **42**, 1464 (1962) [Sov. Phys. JETP **15**, 1016 (1962)].
[77] D. R. Bess and R. A. Broglia, in *Proc. of the S.I.F., Course 69* (Amsterdam, 1977), p. 55.
[78] C. M. Baglin, Nucl. Data Sheets **30**, 1 (1980).
[79] L. Bulboaca, O. Dumitrescu, and M. Horoi, Rev. Roum. Phys. **34**, 469 (1989); in *Proc. of the Roumanian Meeting "Progrese in Fizica"* (ICEFIZ, Bucharest, 1987), p. 92.
[80] J. H. Bjerregaard, O. Hansen, O. Nathan, and S. Hinds, Nucl. Phys. **86**, 145 (1966).
[81] W. McLachtie, W. Darcey, and J. E. Kitching, Nucl. Phys. **A159**, 615 (1970).
[82] G. G. Seeman, J. S. Greenberg, D. A. Brombley, and F. K. McGowan, Phys. Rev. **149**, 925 (1966); R. Diamond, F. S. Stephen, K. Nakai, and R. Nordhagen, Phys. Rev. C **3**, 344 (1971).
[83] J. D. McDougall, W. McLachtie, S. Whineray, and H. E. Duckworth, Nucl. Phys. **A145**, 223 (1970).
[84] S. Hinds, J. Bjerregaard, O. Hansen, and O. Nathan, Phys. Lett. **14**, 48 (1965).
[85] J. R. Maxwell, G. M. Reynolds, and N. M. Hintz, Phys. Rev. **151**, 1000 (1966).
[86] P. Debenham and H. M. Hintz, Nucl. Phys. **A195**, 385 (1972).
[87] B. R. Mottelson and S. G. Nilsson, Phys. Rev. **99**, 1615 (1965).
[88] T. Takemasa, M. Sakagami, and M. Sano, Phys. Lett. **37B**, 473 (1971).
[89] A. B. Migdal and A. I. Larkin, Nucl. Phys. **51**, 561 (1964).
[90] N. Lo Iudice and F. Palumbo, Phys. Rev. Lett. **41**, 1532, 1540 (1978); Nucl. Phys. **A236**, 193 (1979); D. De Francheschi, F. Palumbo, and N. Lo Iudice, Phys. Rev. C **29**, 1496 (1984).
[91] U. E. P. Berg and U. Kneissl, Ann. Rev. Nucl. Part. Sci. **37**, 33 (1987).

Translated by Julian B. Barbour